Studying the Role of Sirtuin-1 Gene in the Maintenance of Mouse Intestinal Epithelium

BY

Emir Sadi Cansu

Thesis completed to meet the requirements for acquiring a degree of

Master of Science in Translational Medicine

at the

University of Helsinki

2015

Table of Contents

Faculty of Medicine	Master's Degree Programme in Translational Medicine	
Subject: Translational medicine	Master's thesis	
Author Emir Sadi Cansu		
Title Studying the Role of Sirtuin-1 Gene in the Maintenance of Mouse Intestinal Epithelium		
Supervisor Pekka Katajisto	Month and year February 2015	Number of pages 94
Supervisor's affiliation Academy Research Fellow, Group leader		

Abstract

Sirtuin-1 (Sirt-1), an NAD^+-dependent deacetylase, maintains energy homeostasis upon stress-induced decline in energy levels. Sirt-1 possesses many other functions ranging from regulating cellular proliferation and apoptosis to maintaining glucose and lipid metabolism. By deacetylating its target proteins, Sirt-1 can also increase the lifespan of lower organisms such as yeast, flies, and worms. However, lifespan-prolonging ability of Sirt-1 in rodent models and human subjects has been investigated, exhibiting only partially promising results.

Contrary to its role in increasing lifespan in rodents and humans, Sirt-1 has exhibited positive results on prolonging the health-span of these model organisms by delaying or inhibiting the development of diseases and disorders that present themselves with increasing age. Drug mediated Sirt-1 activation via resveratrol and Sirt-1 activation through calorie restriction were shown to bring a healthy balance to glucose and lipid metabolism especially in rodents fed on high-fat diet. Currently, Sirt-1 is investigated as a target gene for the treatment of Type-2 Diabetes in multiple clinical trials.

In this study, we investigated the role of the Sirtuin-1 in the maintenance of intestinal epithelium. In our study, we utilized intestinal organoid models grown from isolated crypts of mouse small intestine. We performed knockdown of Sirt-1 at mRNA level via lentiviral shRNA. Additionally, we targeted Sirt-1 activity by applying resveratrol to the culture media of mouse intestinal organoids. Our main aim was to address how manipulations of Sirt-1 expression or activity would affect the function of intestinal stem cells and Paneth cells located in the crypt tips of intestinal organoids. Furthermore, we were interested in how these changes would alter organoid viability and crypt regeneration.

In this study, we demonstrate that Sirt-1 is a fundamental gene for mouse intestinal organoid viability as well as organoid crypt regeneration. We also show that Sirt-1 controls crypt regeneration by regulating Paneth cell differentiation and thus intestinal stem cell niche conditions in the crypt bottoms of mouse intestinal organoids.
Activation of Sirt-1 by resveratrol decreases total Paneth cell number in a crypt bottom leading to the relative retardation of crypt regeneration as well as the reduction in crypt size. High concentrations of resveratrol resulted in death of intestinal organoids, probably due to complete loss of Paneth cells.

Keywords : Sirtuin-1, Crypt, Organoid, Intestine, Lentiviral, Resveratrol, Regeneration, Aging

Where deposited

I. Abbreviations

Akt: Protein kinase B

AMP: Adenosine monophosphate

AMPK: AMP-activated protein kinase

APC: Adenomatous polyposis coli

BMP: Bone morphogenetic protein

BSA: Bovine Serum Albumin

cAMP: Cyclic adenosine monophosphate

CR: Calorie Restriction

DMEM: Dulbecco's Modified Eagle Medium

DR: Dietary Restriction

EB: Ethylium Bromide

EDTA: Ethylenediaminetetraacetic acid

EGF: Epidermal Growth Factor

FOXO: Forkhead Box O

GH: Growth hormone

GSK-3β: Glycogen synthase kinase- 3-beta

HEK293T: Human embryonic kidney 293 T cell line

IGF-1: Insulin-like Growth Factor-1

IIS: Insulin/IGF-1 Signaling

ISC: Intestinal Stem Cell

Km: Michaelis constant

Lgr5: Leucine-Rich Repeat Containing G Protein-Coupled Receptor 5

MES: 2-(*N*-morpholino)ethanesulfonic acid

miRNA: microRNA

mTDNA: Mitochondrial DNA

mTOR: Mammalian target of rapamycin

mTORC1: mammalian target of rapamycin complex 1

mTORC2: mammalian target of rapamycin complex 2

NAD: Nicotinamide adenine dinucleotide

NADH: Reduced nicotinamide adenine dinucleotide

NF-κB: Nuclear Factor Kappa from B cells

NIH 3T3: Mouse embryonic fibroblast cell line

P/S: Penicillin/Streptomycin

PBS: Phosphate Buffered Saline

PGC-1α: Peroxisome proliferator-activated receptor gamma coactivator 1-alpha

PI3K: Phosphatidylinositol 3-kinase

PVDF: Polyvinylidene difluoride

Sir2: Silent Information Regulator-2

SIRT1: Sirtuin-1

SIRT3: Sirtuin-3

SIRT6: Sirtuin-6

STAC: Sirtuin-1 Activating Compound

TB: Terrific Broth

TBS: Tris Buffered Saline

TBST: Tris Buffered Saline + Tween 20

ULK1: Serine/threonine-protein kinase ULK1

VA: Valproic Acid

1. Review of Literature

1.1. Aging

Aging is the progressive decline of physiological integrity in an organism. The decline is manifested by weakening of organ systems resulting in an increased susceptibility to death. Aging also produces the greatest risk factor for the development of pathologies such as cancer, diabetes, cardiovascular disorders, and neurodegenerative diseases.[1] The nature of aging is regulated by genetic factors and biological pathways. By targeting molecules functioning in these pathways, scientists were able to discover that the rate of aging can be controlled exogenously to some extend.

In time, cells accumulate genetic damage and this damage manifests phenotypic characteristics on the organism, which is basically named as aging. Slowing down the rate of genetic damage accumulation in cellular DNA or inhibiting the effects of these damages can make it possible to diminish the biological impact of aging on an organism. Lopez-Otin et al identified nine hallmarks of aging as the main contributors to this phenomenon.[1] Each of these biological concepts has to meet three main criteria to be considered as a hallmark. It should first manifest during normal aging process. When exacerbated in an experimental setting, it should also accelerate aging. Finally, it should also be able to slow down aging when it is experimentally ameliorated. However, third criterion is not so strict as some of these hallmarks have not yet exhibited a potential in slowing down aging and increasing lifespan in experimental settings.[1] According to this three criteria the selected hallmarks of aging are as follows: genomic instability,

telomere attrition, epigenetic alterations, loss of proteostasis, deregulated nutrient sensing, mitochondrial dysfunction, cellular senescence, stem cell exhaustion, and altered intercellular communication.[1] This thesis will touch upon a few of these hallmarks.

1.1.1. Genomic Instability increases with Age

Nuclear and/or mitochondrial DNA can accumulate genetic damage, which affect the rate of mammalian aging and the susceptibility of mammals to develop aging-associated pathologies. DNA damage accumulation at abnormal levels can be the causative factor for the occurrence of premature aging.[2]

Most of the accumulated genetic mutations that damage nuclear DNA are in the form of somatic mutations.[3] Other forms of errors that cause damage are chromosomal aneuploidies and copy number variations.[4-5] These abnormalities have also been discovered as associated with mammalian aging. Damage in critical genes and transcriptional pathways can impair the proper functioning of cells. If these cells are not destroyed through the mechanisms of natural killing such as apoptosis, they may also alter the structure and the function of the tissues they belong to.

When there is an error in replication of cellular DNA, repair mechanisms come into play and manage to correct this error, inhibiting the formation of a new DNA with undesired genetic alteration. However, if the components of DNA repair mechanisms are altered or left partially or completely dysfunctional due to damage, this leads to accelerated DNA damage accumulation and observed as augmented aging phenotype.[1] This phenomenon has been observed in mice models and also explains the development of

some of the human progeroid syndromes such as Werner syndrome and Bloom syndrome.[6-7]

Alterations in the coding sequence of mitochondrial DNA (mtDNA) also affect the rate of aging.[8] Most of these alterations, in the form of genetic mutations, are usually caused by early-in-life replication errors. Some of mtDNA mutations can lead to human multisystem disorders and faster aging. Studies that were performed with mice lacking mitochondrial DNA polymerase γ have shown that these mice exhibit the characteristics of premature aging.[9] Lifespan of mice was also found to be reduced due to the accumulation of point mutations and deletions in mtDNA.[9] Research is now focused on reversing this premature aging process by targeting the mutations in mtDNA in order to observe if mice lifespan can be extended.[1]

1.1.2. Epigenetic Modifications play a key role in Aging

Changes in epigenetic modifications can highly affect mammalian aging and rate at which aging-associated diseases advance. Epigenetic modifications may include DNA methylation, histone modification, and chromatin remodeling.[107] Conservation of epigenetic patterns native to the organism's physiology is maintained by a set of enzymes, which consists of DNA methyltransferases, histone acetylases, deacetylases, methylases, demethylases, and chromatin remodeling protein complexes.[1] Alterations in these enzymes can improve or vanish the ability of the organism to conserve the epigenetic patterns leading to increases or reduction in lifespan. Deletion of histone methylation complex components has been shown to extend lifespan in nematodes and flies.[10-11] Inhibition of histone demethylases in worms has the potential to increase

lifespan through its impact on longevity pathways such as insulin/IGF-1 signaling pathway.[12]

NAD^+ dependent deacetylase coding genes Sirtuins have also been shown to possess potential in affecting organismal longevity.[1] Sirt1, a member of sirtuin gene family, is the closest homolog of Sir2, which was found to increase replicative lifespan of *Saccharomyces cerevisiae* when overexpressed.[13] Following research was done to show that Sir2 homologs sir-2.1 and dSir2 could also increase the lifespan upon activation in worm and fly respectively.[14-15] However, these results were later challenged and that the previous findings on the role of Sir2 homologs in prolonging lifespan were found to be the result of confounding genetic background differences instead of gene overexpression.[16]

Sirtuin genes definitely play a role in improving several of phenotypic outcomes resulting due to aging in rodent models. While overexpression of SIRT1 is found to have no direct effect on rodent aging, it still prevents/slows down the development of aging-associated diseases.[17] SIRT1 activation functions as a protective barrier against the advancing of age-related pathologies through its ability to improve genomic stability and metabolic efficiency.[18-19]

SIRT3 and SIRT6, other genes of sirtuin family, can enhance overall health and/or longevity of mice by using epigenetic mechanisms.[1] SIRT6 has been shown to regulate genomic stability, NF-κB signaling, and glucose homeostasis through histone H3K9 deacetylation.[20-22] Mice deficient in SIRT6 were found to be experiencing accelerated aging.[23] In parallel to this finding, mice overexpressing SIRT6 exhibited longer lifespan compared to control mice.[24] SIRT3, located primarily in mitochondria, has been shown

to mediate the beneficial effects of calorie restriction on the lifespan of mice by deacetylating mitochondrial proteins.[25]

Transcriptional alterations are also seen with increasing age.[26] Microarray studies show clear differences in mRNA levels between young and old tissues of same species. Age-related transcriptional alterations can occur in genes, which code for proteins that function in inflammatory, mitochondrial, and lysosomal degradation pathways.[27] Changes in transcriptional levels in an aging organism can also be seen in non-coding sequences, especially in miRNAs. miRNAs are known to be closely associated with aging and their activity can influence the rate of aging of an organism. miRNAs achieve this ability by targeting proteins that function in longevity pathways or by affecting stem cell behavior.[28-30]

1.1.3. Decline in Proteostasis is seen in Aging Mammalians

Degree of impaired protein homeostasis or proteostasis is another factor that affects the rate of mammalian aging.[31] Cellular proteins go through quality control processes, which check the functional and structural integrity of the proteins. These processes maintain and ensure that proteins translated are folded properly so that they can function in their assigned biological mechanism(s). Proteostasis is the concept of stabilizing correctly folded proteins and degrading some of the misfolded proteins.[1] Proteostasis also functions to restore the misfolded proteins, if not direct them for degradation.[1] This function prevents the accumulation of misfolded proteins as well as protects and stabilizes the properly folded ones inside the cells.

Aging is a natural phenomenon that impairs proper functioning of proteostasis.[32] When proteostasis is not maintained, accumulation of misfolded proteins might be toxic to the organism and it can lead to age-associated diseases such as Alzheimer's disease and Parkinson's disease in humans.[31]

1.1.4. Reduction in Intrinsic Nutrient Sensor Activity Slows Down Aging

1.1.4.1. Insulin and IGF-1 Signaling (IIS)

Anabolic signaling maintained by one of the most evolutionarily conserved pathways of evolution, insulin and IGF-1 signaling (IIS) pathway, accelerates aging.[1] Main targets of this pathway responsible for informing the cells on the presence of glucose are the transcription factors belonging the FOXO family and the mTOR complexes, which were also shown to have an impact on aging.[33-34] Genetic manipulations or activity reducing mutations that occur in the coding sequences of the members of IIS signaling pathway including the growth hormone (GH), IGF-1 receptor, insulin receptor as well as the downstream effectors of this pathway Akt, mTOR, and FOXO were shown to extend longevity in different model organisms.[33-34] In parallel to this finding, dietary restriction (DR) or calorie restriction (CR), which directly reduces activity in IIS pathway, increases lifespan in similar model organisms including but not limited to worms, flies, mice, and non-human primates.[34-35]

Reduction in IIS signaling pathway has direct benefits on organismal longevity. Contrary to this phenomenon, GH and IGF-1 levels were also shown to decline both during normal aging and in mice with premature aging.[36] Thus, constitutive reduction

of IIS extends lifespan whereas reduced IIS signaling is a characteristic of time-dependent physiological aging.

Reason why IIS signaling is reduced in normal aging can be explained as a natural defensive mechanism of organism against aging. IIS signaling is reduced to inhibit or slow down aging, which leads to minimizing cellular growth and metabolism in the circumstance of systemic damage.[37] According to this theory, organisms with a constitutively reduced IIS signaling retain longer lifespan because they possess lower rates of cellular growth and metabolic activity, which is translated to lower rates of cellular damage. Analogous to this biology, physiologically aged organisms try to reduce the activity of IIS signaling pathway in order to extend their lifespan. However, extremely low expression levels of the member genes of this pathway can be lethal to the organism as it will highly reduce cellular growth and inhibit the normal functioning of metabolism. For example, mice with null mutations in either of PI3K or Akt genes die at embryonic stage.[38] Mice with certain progeroid syndromes may exhibit very low levels of IGF-1 and administering IGF-1 can ameliorate premature aging.[39]

Insulin and IGF-1 signaling pathways is linked to three other nutrient sensing pathways. mTOR signaling is used to sense high amino acid concentrations. AMPK and Sirtuins detect low energy state by regulating the levels of high AMP and NAD^+ levels respectively.[1]

1.1.4.2. mTOR

The mammalian target of rapamycin (mTOR) signaling pathway receives intracellular and extracellular signals to regulate cellular growth, proliferation, and metabolism.[40] mTOR pathway functions in many cellular processes including but not limited to insulin

resistance and adipogenesis.[40] In type 2 diabetes and cancer, mTOR signaling pathway can be deregulated. Rapamycin and its analogues are currently being used as active inhibitors of this pathway in treating solid tumors, organ transplantation, coronary restenosis, and rheumatoid arthritis.[40]

mTOR kinase is found in two distinct protein complexes, mTORC1 and mTORC2.[1] Genetically modified yeast, worms, and flies with reduced expression of mTORC1 activity were shown to exhibit increased lifespan, mimicking the similar beneficial effect of CR on lifespan.[41] In mice, rapamycin treatment has also been proven to extend lifespan through the inhibitor effect of the drug on the mTOR signaling pathway.[42] Additionally, increased mTOR activity in mouse hypothalamic neurons caused by aging was shown to promote age-associated obesity.[43] This condition can be reversed by administering rapamycin to mice hypothalamus.[43] Despite the beneficial effects of mTOR inhibition on extending lifespan, severe side effects such as impaired wound healing, insulin resistance, cataracts, and testicular degeneration have been seen in mice models.[44]

High mTOR activity together with IIS signaling pathways can accelerate aging. Opposing to this natural phenomenon, the increased activity in other two nutrient sensors, AMPK and Sirtuins, can extend longevity.

1.1.4.3. AMPK

AMP-activated protein kinase (AMPK) plays significant role in improving lifespan by regulating energy homeostasis, stress resistance, and cellular housekeeping.[45] In studies that were conducted with lower organisms, upregulation of AMPK activity was shown to promote longevity. In mammals, AMPK acts through mTOR signaling to

reduce anabolic programs, and through ULK1 signaling to control autophagy, which enhances the quality of cellular housekeeping and allows redistribution of cellular resources. AMPK activates different signaling pathways including SIRT-1 pathway to improve cellular stress resistance.[45] AMPK signaling declines with aging and its beneficial effects on metabolism disappear. AMPK was shown to inhibit mTORC1 activity, which is an aging enhancing protein complex nucleated with mTOR kinase.[46] AMPK also possesses the ability to activate SIRT-1 in a manner of positive feedback loop[47]; SIRT-1 activated AMPK can further increase SIRT-1 activity and enable SIRT-1 to exhibit its health-promoting effects in the organism. Activated SIRT-1 can deacetylate a wide range of target proteins and directly or indirectly stimulate many different signaling pathways. For example, SIRT-1 can activate PGC-1α, a key molecular complex that control metabolic responses that cause mitochondriogenesis, enhance antioxidant defenses, and improve fatty acid oxidation.[48]

1.2. A Summary on Sirtuin 1 and Its Role in Metabolism

Sirtuin 1 belongs to a family of NAD^+- dependent deacetylases. These enzymes function as cellular sensors by closely regulating energy availability and accordingly modulating metabolic processes. Mammalian SIRT1 protein localized to nucleus is activated upon increases in NAD^+/NADH ratio, which is an indication of low cellular energy state.[49] Activation of SIRT1 causes this enzyme to deacetylate its target proteins leading to the induction of catabolic processes and inhibition of anabolic processes. Mammalian SIRT1 can deacetylate proteins, which possess significant roles in apoptosis, cell cycle, circadian rhythms, mitochondrial function, and metabolism.[19] This ability of SIRT1 enables it to regulate energy storage and in turn provide energy homeostasis in cells

previously experiencing deficiency in energy state. A defect in any of SIRT1 involving pathways can thus cause the disruption of this energy balancing ability of the gene and lead to the development of metabolic disorder in the organism.[19] Activation of SIRT1 on the other hand can be very beneficial as it can be protective against many diseases and disorders such as diet-induced obesity and type-2 diabetes.

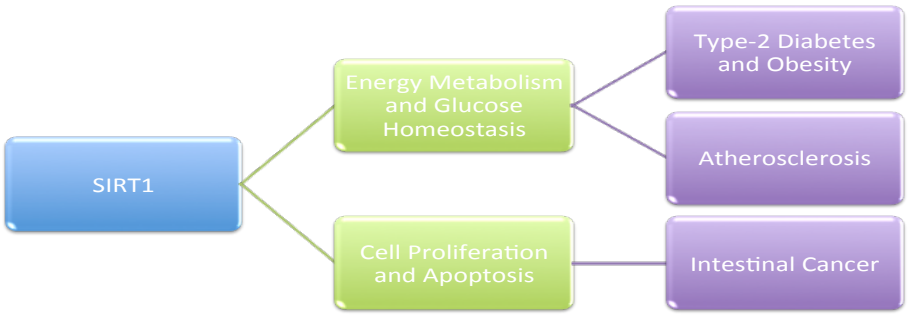

Scheme 1. A diagram exhibiting the importance of SIRT1 on mammalian healthspan. Role of SIRT1 in maintaining energy balance and glucose homeostasis as well as regulating cellular proliferation and apoptosis in mammals significantly affect the development of age-associated diseases such as Type-2 diabetes, obesity, atherosclerosis, and intestinal cancer. Despite the role of SIRT1 in prolonging mammalian lifespan has not yet been proven, part of its impact on mammalian healthspan is exhibited in this diagram.

1.3. SIRT1 as a Target for the Treatment of Diabetes

Sirtuins, a gene family that codes for 7 different NAD+ dependent deacetylases, have a wide range of biological functions. Sirtuin activity has high correlation with Type 2 diabetes.[50] Overnutrition and aging, two main risk factors for diabetes, cause reduced sirtuin activity and lead to abnormal glucose and lipid metabolism.[50] Restoring the function of sirtuins back to their normal levels can be a possible method in treating

Type 2 diabetes. SIRT1, SIRT3, and SIRT6 are the three main sirtuin genes that have exhibited promising potential as drug targets in the treatment of Type 2 diabetes.[50] Sirtuin activators are currently being investigated in clinical trials and their potential to treat Type 2 diabetes as a new alternative approach to already existing treatments has taken significant attention from scientific communities.

SIRT1 is the most studied member of the sirtuin family. SIRT1 is the homolog of Sir2 gene found in lower organisms like yeast, *Caenorhabditis elegans,* and *Drosophila melanogaster*.[13, 15,14] Overexpression of Sir2 gene in these organisms has lead to the extension of their lifespan.[13-15] Considering the fact that SIRT1 is the mammalian homolog of Sir2, scientists have been investigating the possible role of SIRT1 in extending human lifespan. However, the life-extending effects of Sir2 in *C. elegans* and *D. melanogaster* have been called into question, some studies presenting contradictory results on the life-span extending capability of Sir2/SIRT1.[16]

Even though the question whether SIRT1 can extend lifespan in mammals has not yet been fully answered, its impact on age-associated diseases, like Type 2 diabetes, has been brought into light.

1.4. SIRT1 Expression as a Link Between Obesity, Aging, and Type-2 Diabetes

SIRT1 is expressed in many different tissues such as liver, muscle, adipose tissue, heart, pancreas, and brain.[51, 52] However, expression of this gene is not always stable as it can go down with increasing age and many other factors can play into the expression levels

of SIRT1 in different tissues. For example, mice with diet-induced obesity exhibit reduced SIRT1 levels.[53] Humans who are morbidly obese also exhibit reduced SIRT1 levels in visceral adipose tissue.[54] Mice possessing moderate whole-body decrease in SIRT1 eventually develop obesity and insulin resistance[55], and they have elevated lipid accumulation in liver and inflammation in adipose tissue when they are fed on high-fat diet.[60] In parallel with this finding, mice with whole body overexpression of SIRT1 are leaner and more metabolically active, eat less, have decreased fasting serum insulin, glucose and cholesterol, and possess improved glucose tolerance.[57]

1.5. SIRT1 can be Activated by Resveratrol

The role of Sirtuin 1 in maintaining a healthy glucose and lipid metabolism in humans have lead to the search of a novel therapeutic drug which can be utilized to activate SIRT1 and increase its expression levels as a preventive treatment method against Type-2 diabetes and other aging-associated diseases. Resveratrol, found in the nature in the roots of white hellebore plant, *Veratrum grandiflorum*, has been widely used in traditional Japanese and Chinese medicine in curing hyperlipidemia, which translates into high cholesterol and triglyceride levels in blood, one of the main causative factors for developing atherosclerosis.[58, 59] Hyperlipidemia lowering effect of resveratrol has been proven scientifically since resveratrol has shown to reduce lipid accumulation in rats fed on high-fat diet.[60] Resveratrol has also been discovered in red wine.[61] This discovery has taken significant attention because resveratrol could be the answer to the French paradox, which arises from the fact that French consume high amounts of saturated fats yet they exhibit one of the lowest rates of cardiovascular disease.[50]

Resveratrol has later been used to answer one of the most intriguing questions about SIRT1: Can SIRT1 increase lifespan upon its activation with resveratrol? Resveratrol has yet to show any positive effect on increasing the lifespan of healthy mammals under normal conditions. However, administration of this drug restored the lifespan of mice fed on high-calorie diet.[62] Resveratrol has also been shown to possess many antidiabetic effects in rodents. By activating its target gene SIRT1, resveratrol can reduce circulating glucose and insulin levels, improve glucose tolerance, and increase insulin sensitivity.[62-65] Resveratrol has also been successful in reducing blood glucose levels in rodents with β-cell toxin streptozotocin induced diabetes.[66] Resveratrol has also been shown to reduce hepatic lipid accumulation in rodents fed on high-calorie diets.[67]

Despite the wide use of resveratrol in rodents in diabetes and lifespan context, effect of this drug and its potential use as an antidiabetic and/or lifespan prolonging treatment has not yet fully explained. According to the first International Conference on Resveratrol and Health held in 2010, scientists have concluded that the administration of resveratrol to humans as a drug therapy cannot yet take place since there is not yet enough scientific evidence on its role as a disease treating drug.[68] In the studies conducted by Elliott et al. resveratrol was successful in decreasing fasting glucose, postprandial glucose, and postprandial insulin levels in Type 2 diabetic patients.[69] In a study done by Yoshino et al, treating non-obese women with normal glucose tolerance with 75 mg/day resveratrol for 12 weeks exhibited no effect on insulin sensitivity.[70]

Poulsen et al reported that resveratrol, used as a treatment method on obese but otherwise healthy men, had no effect on body composition and insulin sensitivity of the subjects.[71] On the contrary, Timmers et al performed a similar study where resveratrol was shown to increase intramyocellular lipid levels but at the same time decrease hepatic lipids, circulating glucose, insulin, leptin, and improved insulin sensitivity.[72] The contradiction between the results of the two studies mentioned above might have arisen from the difference in study designs, doses of resveratrol administered, and/or the low number of subjects participated in the studies.[50] However, it is definite that more studies and clinical trials are needed before resveratrol can be justified as a safe and efficient drug treatment method for Type 2 diabetes. Both in rodent and human models, resveratrol has minimal or no effect on glucose and lipid metabolism in healthy subjects.[50] In studies where subjects are fed on high-fat diet it has been shown multiple times that resveratrol in higher doses has more potential in reducing body weight.[50] However, the weight lowering effect of resveratrol in high doses has also been accompanied by gastrointestinal symptoms such as nausea and diarrhea.[73]

In general, resveratrol has shown promising results as a novel therapeutic antidiabetic treatment. However, it still requires further clinical studies for the determination of the correct dosing taking into account its pharmacogenetic properties. The indirect effects of resveratrol also need to be addressed in clinical settings, as the drug may have undesired nonspecific effects. Additionally, more specific SIRT1 activators may also be preferred over resveratrol in order to generate better-targeted activation and eliminate possible unwanted side effects in treating Type 2 diabetes.[50]

It is not yet clear whether resveratrol directly activates SIRT1 or its impact on metabolic pathways indirectly cause the activation of this gene. Resveratrol was reported to activate SIRT1 in vitro by lowering its Km for substrate.[74] In a study performed by Park et al, resveratrol was suggested to activate SIRT1 indirectly by binding to phosphodiesterases and triggering cAMP signaling, causing the activation of SIRT1.[75] Other studies have reported evidence on direct activation of SIRT1 by resveratrol. Price et al showed that the acute deletion of SIRT1 in adult mice inhibited the physiological effects of resveratrol, which indicates that these effects are mediated through SIRT1 protein activity.[47] In addition, single point mutation in SIRT1 gene was found to destroy the SIRT1 activating ability of resveratrol as well as of all other 117 synthetic SIRT1 activating compounds (STACs).[76] This point mutation has most probably altered the structure of the allosteric site of SIRT1 enzyme, which inhibited the binding of the enzyme to its activators such as resveratrol.

1.6. Effect of Calorie Restriction on SIRT1 Activity and Aging

Calorie or dietary restriction (CR) has been shown to extend life span in rodent models.[77] This effect of CR on aging of organisms is believed to be mediated by the nutrient sensor genes, the sirtuins. Calorie restriction activates sirtuins, including SIRT1, and leads to its health promoting outcomes as stated in previous chapters. Resveratrol is at the center of scientific attention and currently being investigated in clinical trials as a drug that mimics the sirtuin activator effect of CR.

In previous studies, CR in the form of 30-40% reduction in the ad libitum levels of chow intake was shown to extend lifespan in rodents.[78] In yeast, reducing glucose supply

from 2% to 0.5% was also found to be increasing the replicative lifespan of the organism.[79] However, this extension in lifespan vanishes when SIR2 is knocked out from yeast genome[79], which is a significant indication of the role of SIRT1 homolog SIR2 in aging of the organism. SIR2 independent lifespan extension pathways have also been discovered in yeast models in situations where limitations in glucose level supply was much more severe.[80]

CR studies using mice models are preferred over similar studies including lower organisms as the dietary restriction can be more standardized.[77] In most of the experiments, C57BL/6 mice are fed with 30% reduction of the ad libitum consumption of chow food.[77] In these studies, CR activates sirtuins- predominantly SIRT1- and increases their expression levels. When mice are fed with diet rich in fat, SIRT1 function is lost in mice.[81] Obesity has the similar effect in humans, where SIRT1 function and expression levels can go down in visceral adipose tissue especially in morbidly obese individuals.[82] Genetic modifications in SIRT1 also alter the effect of CR in rodents. For example, knocking out SIRT1 in mice prevents the improvement in physical activity mediated by CR.[83] Transgenic overexpression of this gene also mimics the health promoting benefits of CR. Overexpression of SIRT1 was shown to alleviate the health condition of mice with diabetes, neurodegenerative diseases, liver steatosis, bone loss, and inflammation.[62, 84, 57, 85, 17, 86]

1.7. Mammalian Intestinal Epithelium and Organoid Biology

Intestinal epithelium is composed of a single-cell layer consisting of two main structures: crypts and villi.[87] Intestinal stem cells (ISC) are located in crypts, more specifically at the crypt bottoms.[104] These stem cells function as progenitors for intestinal secretory and absorptive cells. ISCs are positive for Leucine-rich repeat-containing G-protein coupled receptor 5 ($Lgr5^+$ cells) and divide approximately once in 24 hours. Their progeny will continue dividing for few divisions and form the so-called Transient Amplifying pool of cells (TA cells). Simultaneously to cell divisions, the TA cells will progressively differentiate into mature cells of intestinal epithelium as they migrate upwards along the crypt-villus axis, and will stop dividing. Well-controlled differentiation is necessary for intestinal functions such as the maintenance of microbial barrier by mucus and defensin secretion, and for absorption of water and nutrients.[88] $Lgr5^+$ intestinal stem cells are located between Paneth cells in intestinal epithelium. Paneth cells provide the specific niche conditions that are required for the viability and self-renewal of ISCs.[105] Paneth cells also input biological signals to ISCs, which keep the latter in the stem-like state and inhibit undesired differentiation.[87] $Lgr5^+$ stem cells can be isolated from the small intestine of mice either as single cells or as part of intestinal crypts. When cultured in vitro, these cells form organoids, which are living forms that possess an intact lumen in the form of crypt-villi units.[103]

Organoids can grow in vitro with continuous division and differentiation of $Lgr5^+$ ISCs into mature cells of intestinal epithelium.[87] Intestinal crypts isolated from small

intestine of mice can be embedded in Matrigel and cultured in the presence of epidermal growth factor (EGF), R-Spondin, Noggin, N2, NAC, and B27 molecules diluted in DMEM/F12 media containing Glutamax. These organoid growth-promoting factors, collectively known as ENR, provide the cues necessary for organoid development but they are not sufficient in promoting the stem-like state of $Lgr5^+$ ISCs because the self-renewal and differentiation of $Lgr5^+$ ISCs is dependent on direct contact with Paneth cells.[87] $Lgr5^+$ cells cannot be cultured in vitro without the presence of Paneth cells, as the former immediately differentiate into cells of intestinal epithelium. Self-renewal and differentiation of $Lgr5^+$ stem cells are controlled mainly by Wnt, Notch, and bone morphogenetic protein (BMP) pathways.[87] In a previous study, two molecules that target these pathways in single $Lgr5^+$ stem cells and intestinal organoids and maintain the stem-like state of $Lgr5^+$ stem cells were identified.[87] These two compounds, CHIR and Valproic Acid, have enabled scientists to control the differentiation of the stem cells and eliminate the effective role of Paneth cells in this phenomenon.

1.8. Wnt Signaling, SIRT1, Intestines, "Stemness", and Cancer

1.8.1. Wnt Signaling and SIRT1

Wnt signaling regulates adipogenesis, tumorigenesis, and stem cell pluripotency.[89] Wnt ligands transmit signals by activating Frizzled receptors, complex receptors that cross the plasma membrane multiple times.[89] Activation of this set of receptors enables signal propagation inside the cells with the help of Dishevelled proteins and β-catenin molecules in a downstream manner. β-catenin-dependent signaling in which

Dishevelled proteins transfer the signal from Wnt ligands to β-catenin molecules is called canonical signaling.[89]

In the absence of Wnt signaling, glycogen synthase kinase- 3β (GSK-3β) phosphorylates several proteins that favor cellular proliferation, including β-catenin, tagging them for destruction.[90] In the presence of Wnt ligands, activation of Frizzled receptors initiate an intracellular signaling cascade that inhibit GSK-3β activity and indirectly permitting growth- promoting proteins to stimulate cellular growth.[90]

SIRT1, NAD^+-dependent deacetylase, was previously shown to control this Wnt signaling pathway by directly regulating Dishevelled protein levels.[89] SIRT1 loss of function was shown to reduce intracellular levels of Dishevelled proteins.[89] Inhibiting SIRT1 function was also demonstrated as a blockade against Wnt-stimulated cell migration.[89]

1.8.2. Wnt Signaling and APC gene in Intestines

Another regulator of Wnt signaling pathway is the product of the Adenomatous polyposis coli –gene (APC).[90] APC controls cellular proliferation in the whole intestine. Induced by high level of Wnt signals at the crypt bottom, intracellular β-catenin promotes the self-renewal and "stemness" of intestinal stem cells.[90] As the ISCs divide, their previously produced progeny is pushed upwards within the crypt.[90] Cells higher up in the crypt do not receive as many Wnt signals as at the crypt bottom, and intracellular β-catenin levels fall steeply. As a result, these cells lose their stem cell

phenotype, exit the cell cycle, and differentiate into functional intestinal cells of either the secretory or absorptive lineage.[90]

APC is a gene that negatively controls intracellular β-catenin levels in intestinal epithelial cells.[90] APC gene is expressed in undetectable levels in the cells located at crypt bottoms, which also leads to high intracellular β-catenin levels inside the intestinal stem cells.[90] If Wnt ligands are absent, reduction in β-catenin levels increases even more leading to the cellular differentiation of the stem cells into mature cells of intestinal epithelium.[90]

1.8.3. Link between SIRT1, APC, Wnt Signaling, and Intestinal Cancer

Over-activation of Wnt signaling pathway in intestines has been linked to the development of colon cancer.[91] This over-activation might cause the formation of benign tumors in the beginning. Accumulation of additional genetic damage, which may arise due to aging, advances benign intestinal polyps into malignant tumors.[91] SIRT1 has been identified as a target gene that plays a key role in tumor formation in intestines.[92]

In previous research, SIRT1 has exhibited both tumor-suppressive and tumor-promoting roles in intestines of mice models.[93, 94] Global deletion of SIRT1 in $APC^{+/min}$ mice was shown to assign a tumor-promoting role for SIRT1; whereas enterocyte-specific overexpression of SIRT1 led to the conclusion that SIRT1 was a tumor-suppressive gene.[92]

Leko et al, tried to find an explanation to this contradiction. $APC^{+/min}$ mice were crossed with mice possessing enterocyte-specific inactivation of SIRT1 to observe intestinal polyp formation in the offsprings. $APC^{+/min}$ mice demonstrate primary phases of colon cancer in humans and this model is widely preferred to study the impact of candidate tumor suppressor genes and oncogenes on the development of intestinal tumors.[95] Heterozygous $APC^{+/min}$ mice inherit a nonsense mutation in one allele of APC and later lose the wild type allele after birth, leading to the constitutive activation of Wnt-signaling pathway element β-catenin and the formation of multiple intestinal polyps.[96, 97]

Overexpression of SIRT1 only in the intestinal epithelium of $APC^{+/min}$ mice resulted in the formation of fewer intestinal polyps, which was explained as increased deacetylation and nuclear exclusion of β-catenin.[98] However, since overexpressing SIRT1 to levels that are several fold higher than normal physiological levels can mimic gene loss-of-function, the effect of SIRT1 deficiency on polyp formation in $APC^{+/min}$ mice was also studied.[92] $APC^{+/min}$ mice with global SIRT1 deletion developed similar numbers of polyps as $APC^{+/min}$ mice controls.[99] However, mice with global deletion of SIRT1 also exhibited smaller polyps, which indicates that SIRT1 may actually be a tumor promoter.[99] Furthermore, mice with global SIRT1 deletion were shown to express severe growth retardation and reduced blood levels of free Insulin-like Growth Factor I (IGF-I), which is a molecule known for its tumor-promoting ability.[99] Thus, smaller intestinal polyps might be the result of severe reduction in the blood levels of tumor enhancer IGF-I protein not SIRT1.

To study the true effect of SIRT1 deficiency in intestinal polyp formation and resolve the contradicting results previously reported on the role of SIRT1 in tumor development, Leko et al restricted SIRT1 inactivation to intestinal epithelium.[92] In this study, SIRT1 inactivation reduced the total polyp surface, average polyp size, and the number of polyps.[92] SIRT1 inactivation has also caused significant increases in the number of cells experiencing apoptosis, which indicates that SIRT1 functions as a tumor-enhancing gene, promoting the survival of tumor cells in mice intestines.[92]

2. Aim of the Study

The objective of this study is to address if the Sirtuin 1 has a role in homeostatic intestinal stem cell maintenance, and if the Sirtuin 1 activity specifically in the Paneth cells or intestinal stem cells is required for the maintenance of intestinal epithelium. This objective will be addressed by utilizing mouse intestinal organoid models, which form in vitro from isolated crypts of mouse intestinal epithelium.

Furthermore, the link between Sirtuin 1 and crypt growth will be investigated to observe if targeting the Sirtuin 1 could present a novel strategy to alter intestinal regeneration.

3. Materials and Methods

3.1. Preparation of Glycogen Stocks

Bacterial inoculates with five types of plasmids necessary for SIRT-1 gene targeting grown in Carbenicillin/ Terrific Broth media were used to prepare glycogen stocks. 100-µL of bacterial solution was combined with 900-µL of glycogen for each sample and the mixture was then stored at -80 °C.

3.2. Purification of Plasmids of Interest

1-mL of each bacterial inoculate was then transferred into 250-mL of 100 µg/mL Carbenicillin in TB media. The solutions were placed in a mechanical mixer and mixed overnight at 37 °C at 220 rpm. The next day solutions were cloudy, which indicated that the bacteria were able to grow in Carbenicillin /TB media. Each mixture was then super-centrifuged at 10,000g for 10 minutes at 4 °C in order to obtain bacterial pellets.

Plasmids were purified from bacterial pellets by using the NucleoBond® Xtra Plasmid Purification kit from Macherey-Nagel (MN). The bacterial pellets were first suspended in 12-mL of resuspension buffer by pipetting the cells up and down. 12-mL of lysis buffer was then added and the solution was mixed gently by inverting the tube 5 times. The mixture was then incubated at room temperature for 5 minutes. 12-mL of neutralization buffer was added to the suspension and the lysate was mixed gently by

inverting it 10 times until the color turned from dark blue to cloudy white. Neutralization at the proper time is very important because prolonged exposure to the lysis buffer can denature and degrade the plasmid DNA and also release contaminating chromosomal DNA into the lysate.[100] Next step was equilibrating a NucleoBond® Xtra Column together with an inserted column filter. The column was first placed under a falcon tube and the filter was equilibrated with 25-mL of equilibration buffer. The buffer was applied to the rim of the filter and column was allowed to empty by gravity.

The precipitate formed after adding the neutralization buffer was removed by centrifugation at 10,000g for 10 minutes. It is very important to remove the precipitate properly since it can clog the column filter during the filtration and reduce the plasmid yield.[100] The lysate cleared from the precipitate was applied to the rim of the column filter and allowed to empty by gravity. NucleoBond® Xtra Column was then washed with 15-mL of equilibration buffer in order to wash out the lysate remaining in the filter. The column filter was discarded and the column was washed with 25-mL of wash buffer. Next step in purification was to elute the plasmid DNA via 15-mL of elution buffer. The eluate was collected and 10.5-mL of room temperature isopropanol was added to the eluate plasmid DNA for precipitation. The mixture was first vortexed and then centrifuged at 15,000g for 30 minutes at 4 °C. After the centrifugation the plasmid precipitated to the bottom of the tube and the supernatant was carefully discarded. The obtained five DNA pellets were washed with 5-mL of room temperature 70% ethanol. DNA pellets washed with ethanol were then centrifuged at 15,000g for 5 minutes at room temperature. Ethanol was then removed completely from the tube with a pipette

and the pellets were let to dry at room temperature for 10-15 minutes. DNA pellets were then dissolved in 1-mL of TE buffer by pipetting up and down. Plasmid concentrations were determined by using a NanoDrop Spectrophotometer.

3.3. Agarose Gel Electrophoresis of Plasmid DNA

1% Agarose gel was prepared by adding 1.5g of solid agarose into 150-mL of 1x Borate buffer. The mixture was microwaved until solution started to boil. Mixture was then cooled down under cold water and placed on the bench for further cooling. Meanwhile, gel electrophoresis casting pieces were set and placed under the fume hood. 3 drops of Ethylium Bromide (EB) were added into the solution under the fume hood upon the cooling of the solution and the solution was swirled and mixed well. Solution was then poured into the electrophoresis cast and let for solidification for 30 minutes. After the gel was solidified, the comb was removed and the gel was placed in the electrophoresis machine already filled with 1x Borate buffer. 8-µL of 1.5kB DNA ladder was carefully pipetted into the first well from the left. 1-µg of each plasmid purified previously was combined with 5-µL of 6x loading dye and mixtures were loaded into the gel wells. The machine cables were connected properly and device was set to running at 120 V for 1 hour at room temperature. After the running was complete, gel was imaged for plasmid bands.

3.4. Packaging of Lentivirus/ Transfection of HEK 293Ts

In Day 1, HEK-293T cells grown in regular DMEM media-1% penicillin-streptomycin (P/S) in 10-cm dish were passaged in a way that they were 70% confluent the next day. In Day 2, 750-µL of OPTI-MEM media were mixed with 750-ng VSVG plasmid, 6.750-µg del-8.9 plasmid, and 7.5-µg of one of the plasmids of interest purified by using the MN MaxiPrep Kit. This step was repeated six times for each plasmid of interest. In another tube, 4.5-mL of OPTI-MEM was mixed with 180-µL of lipofectamine 2000 and the mixture was incubated at room temperature for 5 minutes. 750-µL of OPTI-MEM+lipofectamine 2000 mixture was mixed with 750-µL plasmid mixture. This step was also repeated six times in order to make separate mixture for each plasmid with lipofectamine 2000. 1.5-mL of mixture was then mixed gently and incubated at room temperature for 20 minutes. 1.5-mL of the OPTI-MEM, lipofectamine 2000, and plasmids solution was added to 6-ml of DMEM without P/S. This mixture was replaced with the old media of HEK 293T cells. The new mixture was added dropwise with a 1-mL pipette onto the cells. The cells were kept in an incubator for 48 hours with no change of media.

In Day 4, supernatants were collected from each 10-cm dish and were passed through a 45-µm filter to get rid of the cell debris. Six types of supernatants each containing a different lentivirus were then concentrated by using Lenti-X™ Concentrator from Clontech. 1 volume of Lenti-X™ Concentrator was combined with 3 volumes of viral

supernatant. The solution was mixed gently by inversion and was incubated at 4 °C overnight. Next day samples were centrifuged at 1,500g for 45 minutes at 4 °C. An off-white pellet was visible after the centrifugation. The supernatant was removed and the pellet was resuspended in total volume of 70-µL, which included pellet residual volume and DMEM. The concentrated viral samples were stored at -80 °C to be used for cell infection in the following day.

3.5. Transduction and Selection of NIH 3T3 Cells with Lentivirus

In Day 1, 10-cm plate of mouse fibroblast NIH 3T3 cells were passaged into two 6-well plates in a way that they were 70% confluent the next day. A mixture of DMEM media with P/S, 8-µg/mL polybrene, and 5-µL of one of six concentrated lentiviruses was prepared. The solution was mixed gently by inversion and was used to replace the old DMEM media with P/S. The plates were kept in the incubator for two days. In Day 3, old media was replaced with DMEM media with P/S having 1.5-µg/mL puromycin, the antibiotic for selecting the infected cells. Media with puromycin was kept on the cells for two days. In Day 5, puromycin media was replaced with basic DMEM media with P/S. In Day 6, each type of infected and selected NIH 3T3 cells from one of two wells was lysed for protein quantification and western blotting.

3.6. Sample Preparation for Western Blotting

NIH 3T3 cells recovered from puromycin selection were lysed for Western Blot analysis. First, old regular media was aspirated and the cells were washed with ice-cold PBS. 500-µL of RIPA buffer with 2x protease and phosphatase inhibitors were added on

the cells. Cell scraper was used to collect the lysate into 1.5-µL centrifuge tubes. Cells were kept on ice during the whole process. After the lysates were collected, samples were agitated in the cold room for 30 minutes, which was followed by spinning down at 16,000 g at 4 °C to get rid of the cell debris. Supernatants were then transferred into new eppendorf tubes and the pellets were discarded.

Absorbance measurement was done in order to determine the protein concentration of the lysate samples. BSA (Bovine serum albumin) standard protein assay was used and BSA dilutions of 1 mg/mL, 0.5 mg/mL, 0.25 mg/mL, 0.125 mg/mL, 0.06 mg/mL, and 0 mg/mL were prepared. Both the sample and the standard were diluted with the lysis buffer. 25-µL of sample and standard were added to the plate for absorbance measurement and covered with aluminum foil. Samples were kept at 37 °C for 1 hour and then taken to absorbance reader machine. Absorbance values and BSA-standard linear curve were then used to calculate the protein concentration in the lysate samples. Concentration values were used to calculate the amount of protein to load for Western Blotting analysis.

3.7. Western Blotting with NIH 3T3 Cell Lysates

Total volume of 40-µL of protein from lysed NIH 3T3 cells, 10x reducing agent, 4x sample buffer, and water were prepared and mixed gently by pipetting up and down in the cold room. Heat block was switched on and temperature was set to 70 °C. Samples were incubated at 70 °C for 10 minutes and were put back on the ice immediately after incubation. Samples were centrifuged down briefly and placed back on ice. A Western

Blotting tank was filled with appropriate volume of 1x MES-running buffer and the machine was set for running according to the user guidelines. 40-µL of each sample was loaded into the wells and the sample was run at 165 V for 35 minutes. In between the sample running, two sponges were soaked in the transfer buffer. Two PVDF membranes were soaked first in methanol in a shaker for 1 minute, then in water in a shaker for 5 minutes. PVDF membranes were then transferred into transfer buffer. The machine was set for transferring of protein bands from the Western Blotting gel onto the PVDF membrane. Sponges, gel, and PVDF membranes placed on top of each other according to the user guidelines and the machine was set to 30V and run for 1 hour. In between the transferring, TBST buffer was prepared from 1x TBS buffer with Tween 20 at 0.05% final concentration. 5% milk was then thawed in TBST on ice. After 1 hour of transferring, the membrane was incubated with 5% milk for 1 hour at room temperature in a shaker. The membrane was then washed with TBST once. Anti-Sirtuin-1 rabbit polyclonal antibody purchased from Merck Millipore was diluted 1:500 in 10-mL of TBST-5% milk. The membrane was placed in middle size plastic box and the antibody solution was poured onto the membrane. The box was closed, wrapped with parafilm, and left on a shaker in cold room overnight. In the next day, the antibody solution on the membrane was pipetted out into a tube and placed in a freezer at -20 °C. The membrane was then washed three times with TBST with every washing lasting for 10 minutes. Before the last wash with TBST was completed, anti-rabbit secondary antibody was diluted 1:15000 in 10-mL of TBST-5% milk. The secondary antibody solution was added onto the membrane placed in a shaker box and kept for 2 hours on a shaker at room temperature. After the incubation with the secondary antibody solution,

the membrane was washed again with TBST three times, each wash lasting for 10 minutes. The membrane was then placed on a transparent plastic layer and SuperSignal West Femto® chemiluminescent substrates purchased from Thermo Scientific were added onto the membrane and the membrane was immediately covered with aluminum foil since this step was light sensitive. The membrane was then imaged for Sirt1 bands with Fuji Film Luminescent Image Analyzer LAS-3000. After the imaging was complete, membrane was washed with TBST once and Anti-β-Actin antibody with 1:5000 dilution in 10-mL of TBST-5% milk was added onto the membrane. The box where the membrane was placed was closed and wrapped with parafilm and left on the shaker in cold room overnight. In the following day, the actin antibody solution was pipetted out and the membrane was washed with TBST three times, each wash lasting for 10 minutes. The anti-rabbit secondary antibody solution with 1:15000 dilution in 10-mL of TBST-5% milk was added onto the membrane in a shaker box and left for 2 hours for shaking at room temperature. Membrane was then washed three times with TBST, each wash lasting for 10 minutes. SuperSignal West Femto® chemiluminescent substrates were added on the PVDF membrane and membrane was covered with aluminum foil since the substrates were light sensitive. The membrane was then used to take images of β-Actin bands at different exposures with LAS-3000. Band images at different exposures were then compared and the clearest ones were selected for protein quantification analysis with Image J.

3.8. Isolation of Small Intestinal Crypts from Mice Donors

Mice were first euthanized in $C0_2$ chamber by constant flow of CO_2 into the chamber for 5 minutes. Mice were taken out of the chamber and cervical dislocation was done by applying pressure to the nape of the animal and pulling it from its tail in order to make sure that the animal was sacrificed properly. Small intestine was then removed together with stomach by making two cuts: one around stomach-esophagus connection and one at small intestine-cecum connection. Small intestine was then placed in a 10-cm dish filled with ice-cold PBS. Feces inside the small intestine were removed by injecting PBS into the lumen. Fat and mesentery were also cleaned away by rubbing the intestine with fingers. Intestine was then opened longitudinally and gently rubbed between fingers in cold PBS to remove the mucus. Intestine was cleaned until it appeared pale pink color. Intestine was then cut into approximately 3-mm fragments and the fragments were placed into a 50-mL conical tube filled with 30-mL of ice cold PBS-10-mM EDTA. The tube was shaken intermittently on ice for 45 minutes discarding and replacing the supernatant once every 15 minutes. Fragments were then resuspended with ice cold 30-mL of PBS-10mM EDTA. The tube was incubated on ice for 60 minutes and shaken gently every 10 minutes without changing the supernatant. Contents were then passed through a 70-μm filtering mesh in order to remove villous material and tissue fragments. The filtrate was centrifuged for 6 minutes at 400g at room temperature. The supernatant was discarded and the pellet formed at the bottom of the tube was kept on ice. Pellet was then resuspended in 1-mL of fresh crypt culture media.

3.9. Intestinal Crypt and Organoid Culturing

Crypts isolated from small intestine are resuspended in 1-mL of regular ENR media (see section 3.11 for media ingredients). Matrigel thawed on ice was used together with ENR media for crypt culturing. 30-µL drops containing 60% Matrigel and 40% crypts in ENR media were pipetted carefully to the center of wells of a 48-well plate while keeping the Matrigel and crypts resuspended in media on ice at all times. After the crypts were plated in Matrigel and media drops, the plate was kept in incubator for 20 minutes for the solidification of Matrigel. Later, plate was removed from the incubator and the drops were checked for proper solidification. If the drops were properly solidified, 300-µL of ENR media were added to the walls of each well. The surrounding wells received around 100-300-µL of ddH_20 in order to prevent evaporation of the ENR media.
The next day viable crypts form round organoids if cultured in ENR media with ingredients of proper amount. Organoids were passaged every 2-3 days depending on their growth rate and viability. Surface of the wells were scratched with 1-mL sized pipette tip and the Matrigel was broken and mixed into the culture media. The media were then transferred into a 15-mL tube and the volume was increased to 10-mL by adding PBS. Organoids were then centrifuged for 30 sec at 400g at room temperature. The supernatant was removed until 1-mL of it was left. Organoid pellet at the bottom of the tube was resuspended by pipetting up and down for 10 times. More PBS was added into the tube and the volume was increased up to 10-mL. The organoids were centrifuged again for another time at 300g for 1 minute. The supernatant was pipetted out until 200-µL line. Organoid pellet was resuspended again in 200-µL volume with

200-µL pipette tip by pipetting up and down for 20 times. More PBS was added and organoids were centrifuged for a third and a last time for 3 minutes at 300g at room temperature. The supernatant was then completely removed until only 10-20-µL was left on the organoid pellet. Organoids were then resuspended in desired amount of ENR media and plated as stated above. The continuous centrifuging-resuspending cycle was done in order to break the organoids into small crypts. When organoids are properly broken into crypts, each viable crypt forms a new organoid. Therefore, the whole purpose of passaging organoids is to break them into their smaller crypt units and restart the crypt to organoid growth process, obtaining more organoids.

3.10. Organoid Transduction with Lentivirus

Organoids were cultured for 6 days in regular ENR media containing 1-mM Valproic Acid and 3-µM CHIR compound. Organoids were passaged once in day -2 and media was changed once in every two days. In day 0, lentiviral transduction of organoids with one non-targeting virus and two Sirt-1 knockdown viruses was performed. Organoids were first mechanically detached from Matrigel by using a pipette tip and they were transferred into a 15-mL tube. Volume was increased up to 10-mL with PBS and the organoids were centrifuged for 1 minute at 300g at room temperature. Supernatant was then removed until 1-mL of it was left. The organoid pellet was resuspended by pipetting up and down 10 times with a 1000-µL pipette tip. Second wash with PBS was done and organoids were centrifuged for 2 minutes at 300g at room temperature. Supernatant was removed by suction until only 200-µL volume was left in the tube. Organoids were resuspended again by pipetting up and down 20 times with a 200-µL

pipette tip. PBS was added into the tube to raise the volume to 10-mL. Organoids were centrifuged for the third and the last time for 3 minutes at 300g at room temperature. Almost all of the supernatant was then removed by suction. 120-µL of DNAsI was added to 500-µL TrypLe and the mixture was then added on the organoid pellet. The organoids were pipetted up and down while keeping the tube on ice at all times. Organoids were then placed in water bath pre-warmed to 32 °C and kept in for 120 seconds. Organoids were immediately placed back on ice and resuspended with 12-mL of cold SMEM with 120-µL DNAsI by pipetting up and down for 3 times. Resuspended organoids were then centrifuged for 5 minutes at 400g. Supernatant was discarded and pellet was immediately placed back on ice. Organoid pellet was resuspended with total volume of 125-µL infection media (see Media section for all types of media ingredient details) and virus. Viruses were kept at -80 °C and thawed on ice few hours before infection. 125-µL of DMEM-F12 media was added to the resuspension and the volume was raised up to 250-µL. 250-µL of organoid and virus resuspension was then pipetted to a single well in a 64-well plate. Plate was spinned down for 70 minutes at 600g at 32 °C. Plate was then incubated for 1 hour at 37 °C. Organoids in infection media were then transferred into eppendorf tubes and infection media was discarded after organoids were pelleted by centrifugation for 5 minutes at 300g at room temperature. Organoids were then resuspended in 48-µL culture media and cultured as explained in the Intestinal Crypt and Organoid Culturing section of Materials and Methods. Culture media was changed every day. In day +2, 48 hours after lentiviral transduction of organoids, culture media was replaced with puromycin selection media. Organoid number was counted and images were taken at 5X objective before changing the culture

media to puromycin selection media. Puromycin selection media was kept on the infected organoids for 2 days and in day +4 replaced with media for infected organoids. In day +5, media for infected organoids was replaced with regular ENR media. Media was changed every two days. In day +7, transduced organoids were counted and imaged. Organoids were kept growing in ENR media with media change in every 2 days until day +13. Organoids were checked everyday for organoid bubble structure formation, viability, and crypt budding.

3.11 Media Ingredients for Mouse Intestinal Organoid Culturing and Transducing

Information on intestinal organoid media ingredients is given below. Names of the products, company providers, and serial codes of the products that were used in organoid experiments can be found in the boxes below. Volumes of each ingredient used and their final concentrations in each type of media are also provided.

Substrate Name	Company Provider	Serial Number
DMEM-F12	Invitrogen	12634028
Glutamax	Invitrogen	35050-061
EGF	R&D Systems	AFL-2028
Noggin	Peprotech	250-38
Y-27632	Sigma-Aldrich	Y0503
N2	Gibco	17502-048
B27	Gibco	17504-044
R-Spondin	R&D Systems	3474-RS
Matrigel	BD Biosciences	356231
NAC	Sigma-Aldrich	A9165
CHIR 99021	Biovision	1677-5
Valproic Acid	Cayman Chemicals	13033
Wnt3A	R&D Systems	5036
Jagged 1	AnaSpec	188-204
Nicotinamide	Sigma-Aldrich	N0636
Polybrene	Sigma-Aldrich	H9268
Puromycin	Sigma-Aldrich	P8833

Culture Media for Freshly Isolated Crypts	Volume (uL)	Final Concentration (ug/mL)
DMEM-F12	10000	
Glutamax	100	1x
EGF	1	0.05
Noggin	2	0.1
NAC	10	1uM
N2	100	1x
B27	200	1x
R-spondin	20	0.5
Y-27632 (first 2 days of culture)	10	10uM

Regular Culture Media for Organoids (ENR Media)	Volume (uL)	Final Concentration (ug/mL)
DMEM-F12	10000	
Glutamax	100	1x
EGF	1	0.05
Noggin	2	0.1
NAC	10	1uM
N2	100	1x
B27	200	1x
R-spondin	20	0.5

CV Media for Organoids	Volume (uL)	Final Concentration (mM)
ENR Media	10000	
CHIR 99021	3	0.003
Valproic Acid	55.56	1

Infection Media for Organoids	Volume (uL)	Final Concentration (ug/mL)
Regular ENR media 2x concentrated	500	
Extra R-Spondin	2	1
Wnt3A	1	0.2
Jagged 1	1	20uM
CHIR 99021	1.5	0.003mM
Valproic Acid	5.55	1mM
Nicotinamide	6.17	10mM
Polybrene	4	8

Culture Media for Infected Organoids	Volume (uL)	Final Concentration (ug/mL)
Regular ENR media	2000	
Wnt3A	2	0.1
Y-27632	2	10uM
Jagged 1	2	10uM
CHIR 99021	6.06	0.003mM
Valproic Acid	22.22	1mM
Nicotinamide	24.7	10mM
Extra R-spondin	4	0.5

Puromycin Selection Media for Infected Organoids	Volume (uL)	Final Concentration (ug/mL)
Regular ENR media	2000	
Wnt3A	2	0.1
Y-27632	2	10uM
Jagged 1	2	10uM
CHIR 99021	18.18	0.009mM
Nicotinamide	24.7	10mM
Puromycin	2	2

3.12. Activation of Sirtuin-1 Gene in Intestinal Organoids by Resveratrol

Crypts from a small intestine of a 3-12 months old C57/B6 Lgr5-EGFP-IRES-creERT2 mouse were isolated according to the Isolation of Small Intestinal Crypts protocol explained in detail in the Materials and Methods section. After the isolation, in day 0, crypts were cultured in freshly isolated crypt culture media. In day 1, media was replaced with regular ENR media without Y-compound. In day 2, organoids formed from intestinal crypts were passaged in order to remove the dead cells. In day 3, organoids in each well were counted and images were taken at 5x and 10x objectives. Resveratrol in solid form purchased from Sigma-Aldrich stored at -20 °C was dissolved in pure ethanol and stock concentration of 200-µM resveratrol in Regular ENR Media was prepared. 200-µM resveratrol in ENR Media was diluted to obtain 100-µM and 50-µM resveratrol in ENR Media. ENR Media with same volume of pure ethanol corresponding to different resveratrol concentrations were prepared for control

purposes. Organoids were divided into two main groups: control group receiving ENR media with different volumes of ethanol and experimental group receiving ENR media with different concentrations of resveratrol. It is important to underline that the control organoids were also divided into 3 groups, each group being the control of an experimental organoid group, which received ENR media of 200-µM, 100-µM, or 50-µM resveratrol. In day 3, regular ENR media for six groups of organoids was replaced with ENR media with resveratrol dissolved in pure ethanol or ENR media only with pure ethanol. Organoids were grown in resveratrol for two days and in day 5 surviving organoids were counted and imaged at different objectives in wells that received either resveratrol or ethanol. In day 5, media for organoids was replaced with fresh ENR media with or without resveratrol. In day 6, more images were taken in order to count the average number of crypts per organoid. Images were also used and analyzed in Image J in order to measure crypt lengths and crypt widths. Paneth cells located at the crypt bottoms were counted under Light Microscope at 40x objective and images were taken. Only the crypts that were growing perpendicular to z-plane were included in Paneth cell counting analysis.

4. Results

4.1. Purification of Sirt-1 Plasmids of Interest

Plasmids for targeting Sirt1 gene in intestinal organoids were increased in copy number by bacterial culturing and isolated as stated in Materials and Methods section. Five plasmids with shRNA targeting sequences for Sirt1 were constructed in pLKO.1 backbone as shown in the table below.

Plasmid ID	TRCN ID	Target Sequence in Mouse Sirt1	Vector
B01	TRCN0000039296	GAGGGTAATCAATACCTGTTT	pLKO.1
B02	TRCN0000039297	CCTGAAAGAACTGTACCACAA	pLKO.1
B03	TRCN0000039298	CGCGGATAGGTCCATATACTT	pLKO.1
A11	TRCN0000039294	GCCATGTTTGATATTGAGTAT	pLKO.1
A12	TRCN0000039295	GCCATGAAGTATGACAAAGAT	pLKO.1

Plasmid ID	Concentration (ng/uL)	260/230	260/280
B01	147.5	2.19	1.95
B02	302.3	2.27	1.84
B03	212.8	2.30	1.92
A11	106.5	2.23	1.98
A12	266.3	2.28	1.80

Purified plasmids were measured for their concentration, 260/230, and 260/280 values with Nano Drop spectrophotometer. As shown in the table, purified plasmid DNA meet the purity criteria according to their absorbance values at different wavelengths. This indicates that the plasmids can be used for transfection and Sirt1 targeting lentivirus production.

4.2. Running Plasmid DNAs on Agarose Gel

Plasmids that were shown to be pure from the absorbance values measured by a spectrophotometer, were also run on an agarose gel to see if there were any bacterial DNA contamination. This step was necessary to double prove the purity of the plasmids, which was important for successful transfection and virus production. Isolated plasmids demonstrated expected gel running patterns of closed circular and open circular forms, and were considered sufficient quality for lentivirus production

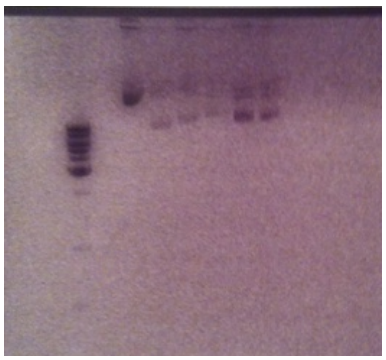

Fig 1. Gel electrophoresis image of plasmid DNAs. From left to right: 1.5Kb DNA ladder, B1, B2, B3, loading error, A11, and A12 plasmids. As seen in the figure provided, all plasmids existed in two different confirmations with no sign of bacterial DNA contamination or plasmid DNA digestion.

4.3. Knocking Down Sirt-1 in NIH 3T3 Mouse Fibroblast Genome by Lentiviral Transduction

NIH 3T3 cells were infected with five different lentiviruses to identify the knockdown efficiency of each virus. An additional control lentivirus was also used to infect NIH 3T3 cells. This lentivirus was a non-specific non-targeting lentivirus, which integrated into a non-coding region in cells genome. After different groups of NIH 3T3 cells were infected with either a control lentivirus or one of five lentiviruses with Sirt1 knocking down potential, cells were grown for 48 hours in vitro. Selection marker puromycin was added in media after 48 hours of growth and was kept on the cells for another 48 hours. Cells, which were not infected by a lentivirus, were not able to survive in the media

containing 1.5-µg/mL puromycin. However, cells which had a lentivirus integrated in their genome were resistant to the killing effect of puromycin since the pLKO.1 backbone in the virus genome had the gene for puromycin resistance. After the puromycin media was taken out, cells were observed to determine percent cell viability. Viability of 80-90% would indicate that the lentivirus had high viral infecting efficiency and could potentially be used for transducing more difficult targets, such as intestinal organoids. Exposure to puromycin for 48 hours almost killed all of the NIH 3T3 cells that were transduced by either B01 or A12 virus. Cells infected with non-targeting, B02, B03, and A11-lentivirus had a surviving rate of approximately 80%, which was determined with an experienced eye. For the western blotting experiment needed for determining the knockdown efficiency of each lentivirus, NIH 3T3 cells transduced with one of the four lentiviruses were used: Non-targeting, B02, B03, and A11. Lentiviruses B01 and A12 were omitted from further experiments since they were not successfully able to infect their target cells.

4.4. Western Blotting of NIH 3T3 Cells Transduced by a Sirt-1 Targeting Lentivirus

Protein concentrations of lysates of NIH 3T3-shRNA-Non-targeting and NIH 3T3-shRNA-SIRT1-KD cells were calculated according to the protocol provided in Materials and Methods section. Absorbance level of each lysate was measured by a spectrophotometer and the protein concentrations of cell lysates were determined by using BSA protein linear-fit standard curve as shown in the table below.

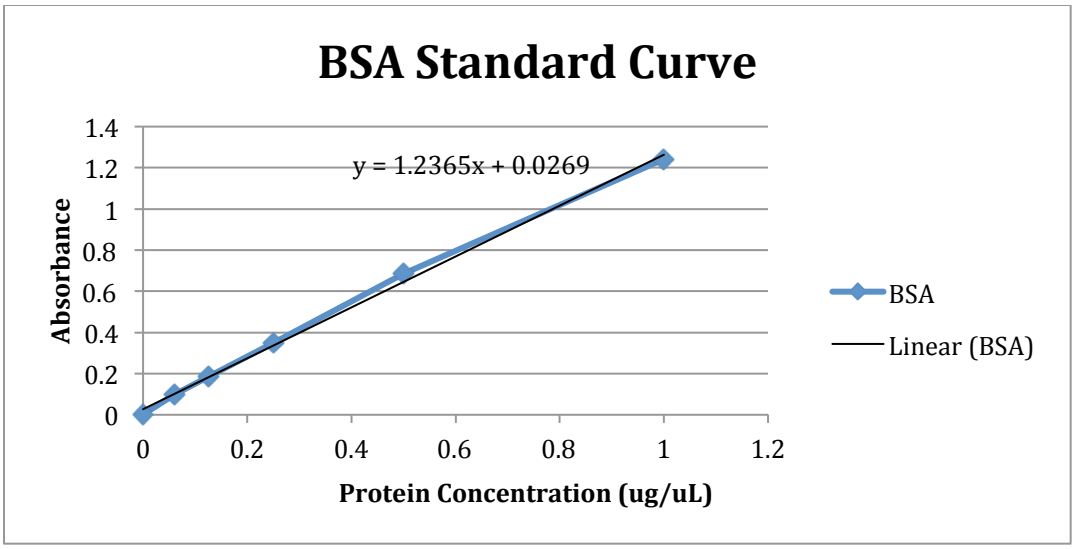

Logic behind using BSA standard curve is as follows: BSA samples with pre-known range of concentrations were used to measure their absorbance. The obtained data was then used to construct a linear fit, which shows a positive linear correlation between protein concentration and absorbance. Below are the protein concentrations of lysates of transduced cells that were calculated by using the BSA standard linear fit equation.

Cell Lysate	Absorbance	Protein Concentration (µg/µL)
sh Non-Targeting	0.702	0.546
sh SIRT1-KD B2	0.57	0.439
sh SIRT1-KD B3	0.558	0.4295
sh SIRT1-KD A11	0.6	0.4635

11.5 µg of protein from the lysates of transduced NIH 3T3 cells were loaded into the Western Blotting lanes and the volume to be loaded was calculated from the protein concentrations.

4.5. Western Blot Image and Analysis of Percent Knock Down of Sirt-1

NIH 3T3 cells transduced with lentiviruses knocking down the expression of Sirt-1 gene at mRNA level via shRNA method were analyzed to determine the knock down efficiency of each lentivirus. Purpose of conducting this experiment was to identify the two most suitable lentiviruses for mouse intestinal organoid transduction, which perform the highest Sirt-1 knockdown levels. Figure 2 below shows the image of SIRT-1 and β-Actin bands on PVDF membrane captured at the optimal exposure time of 20 seconds.

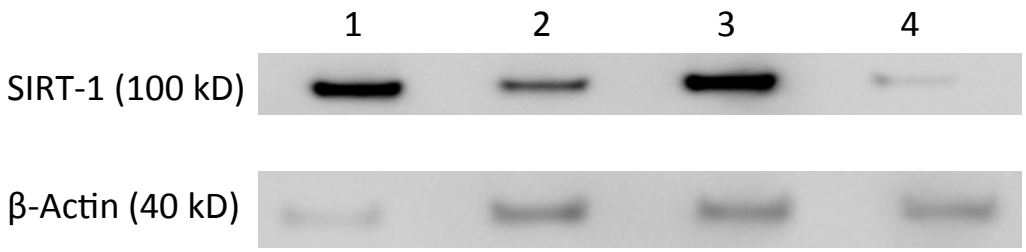

Fig 2. Western Blotting Image of NIH 3T3 Whole Cell Lysates. Sirt1 gene was knocked down in all models. Lane 1 contains proteins from cells transduced with Non-specific Non-Sirt-1 targeting lentivirus. Lane 2 has cellular proteins of Sirt-1 Knocking Down B2-lentivirus. Lane 3 has proteins of cells transduced with Sirt-1 Knocking Down B3-lentivirus. Lane 4 has proteins of cells transduced with Sirt-1 Knocking Down A11-lentivirus. Lanes were analyzed in Image J to determine the two best Sirt-1 knock down models. Western blotting was conducted and images were captured as described in Section 2.7 of Materials and Methods.

In each knock down cell line, it is clear that Sirt-1 gene was knocked down successfully since the ratio of β- Actin/Sirt1 in all Sirt1-targeted cell lines was dramatically lower in cells transduced with the control virus. To quantify the results, Image J program was used: β- Actin levels were normalized and area-under-curve (AUC) of each Sirt-1 band

were multiplied with the normalization factor obtained from the analysis of β- Actin bands. Results from AUC multiplied with normalization factor were then compared to each other. AUC x Normalization factor of control cells were accepted as 100% Sirt-1 expressed (0% knockdown). AUC x Normalization factor of other models were then compared to the value of control cells and percent expression of Sirt-1 gene in NIH 3T3 cells transduced with Sirt-1 knocking down lentivirus was calculated as shown in table below. sh-SIRT-1 B2 and sh-SIRT-1 A11 were chosen for mouse intestinal organoid transduction experiment as these lentiviruses exhibited the two highest Sirt-1 knockdown levels as seen in Figure 3.

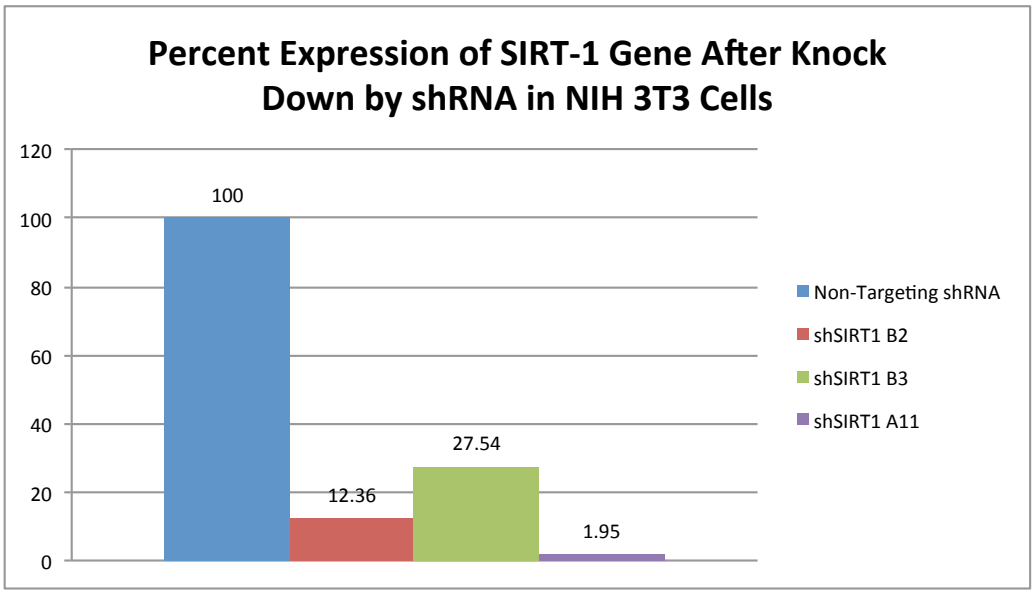

Fig 3. Percent expression of SIRT-1 gene in NIH 3T3 cells after the transduction with SIRT-1 targeting lentivirus. Lane images were analyzed on Image J and β- Actin bands were utilized for normalization purposes. According to the results, shSIRT1 B2 and shSIRT1 A11 lentiviruses exhibited the highest knockdown of the target gene in NIH 3T3 cells.

4.6. Knock Down of Sirt-1 Gene in Mouse Intestinal Organoids by Lentiviral Transduction

Mouse intestinal organoids cultured in CV media for 6 days were transduced with non-targeting, Sirt-1 targeting sh-B2, and Sirt-1 targeting sh-A11 lentiviruses as described in part 3.10 of Materials and Methods section. Intestinal organoids were grown in culture media for infected organoids for 2-days followed by changing the media to puromycin selection media. During the selection, organoids that were disintegrated into single cells or clusters of cells during the infection process started to re-grow into new organoids. Images of re-growing organoids were captured and organoids were counted under the microscope before culture media for infected organoids was changed to puromycin selection media. Fig 4. shows the captured images of organoids with 5x objective just before the addition of puromycin selection media. Two days after the transduction, intestinal organoids that were transduced with different lentiviruses were grown to different sizes. As seen in Fig 4. Intestinal organoids that were infected with a Sirt-1 knockdown lentivirus were much bigger in size compared to the organoids that were either infected with a non-targeting lentivirus or no virus at all.

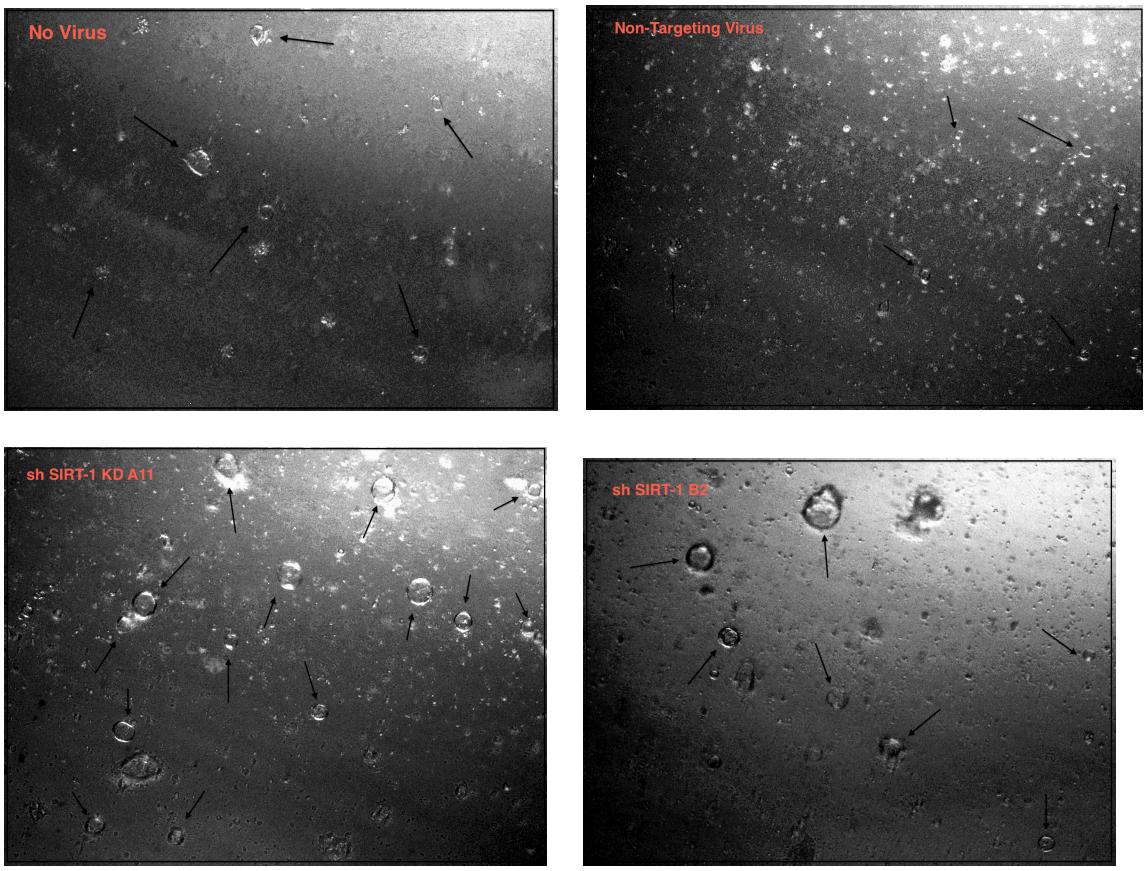

Fig 4. Mouse Intestinal Organoids Two Days Post-Transduction. All images were captured at 5x objective. Organoids, which were exposed to infection process with one of SIRT-1 knocking down lentivirus were bigger in size compared to organoids which were infected with control virus or non-infected organoids. **Note that at this stage it was not yet proven if all these organoids were successfully transduced.**

Two days after puromycin selection media was added, media was changed to regular ENR media and the surviving organoids were grown for three days before counting. Fig 5. shows the percent of organoids surviving 3 days after puromycin selection was complete.

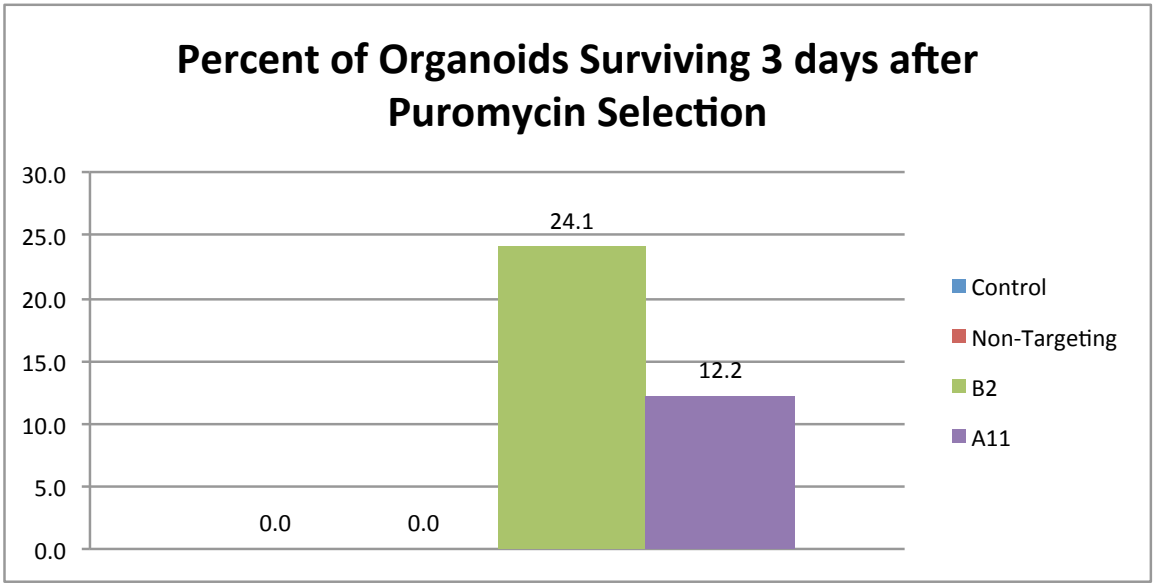

Fig 5. Percent of Mouse Intestinal Organoids Surviving after Puromycin. Organoids were counted just before puromycin selection and 3 days after puromycin selection. No organoids were surviving in non-infected and control virus transduced groups.

As expected, organoids that were not transduced were all dead after they were exposed to media with puromycin since they did not have the resistant gene against puromycin. However, organoids which were transduced with non-targeting control lentivirus were all dead too. This showed that the control lentivirus was not able to successfully infect the mouse intestinal organoids. Organoids, which were infected with a SIRT-1 targeting lentivirus had survival rates in the range of 12-24%.

Fig 6. shows chosen images of organoids that were transduced with a SIRT-1 knockdown lentivirus, 3 days after the puromycin selection was complete.

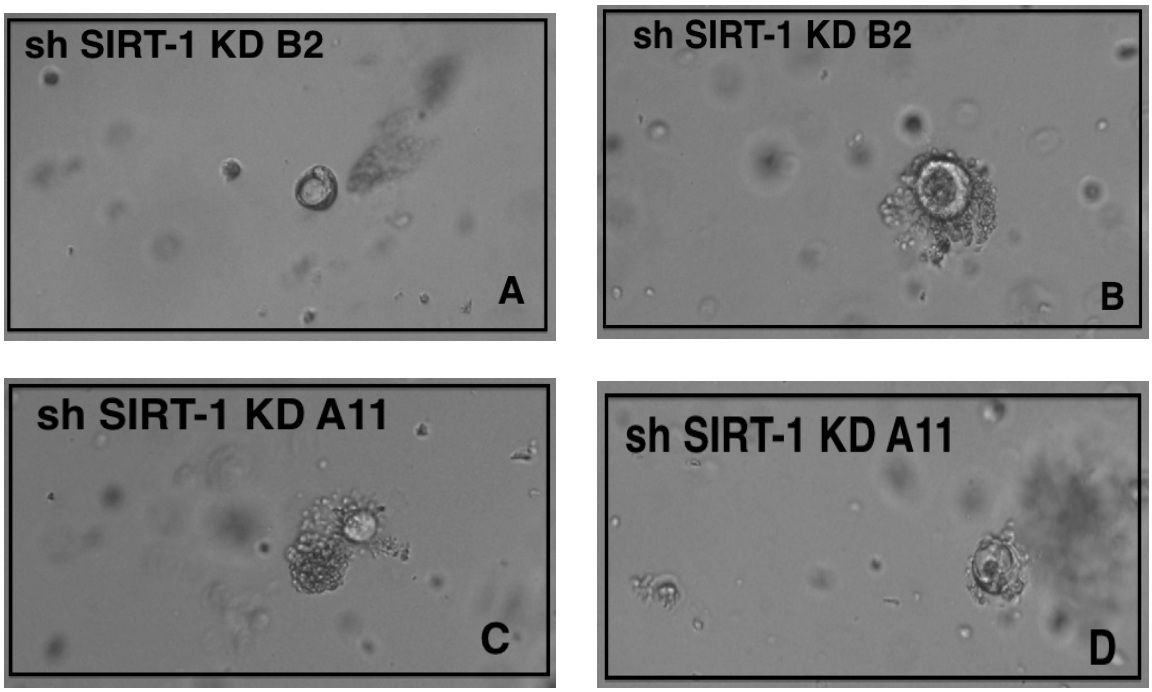

Fig 6. Mouse intestinal organoids transduced with SIRT-1 targeting lentivirus. Organoids were successfully transduced since they were able to survive in media containing puromycin. **A-B.** Surviving organoids transduced with SIRT-1 targeting lentivirus B2. **C-D.** Surviving organoids transduced with SIRT-1 targeting lentivirus A11. Images were taken at 10x objective.

Intestinal organoids shown in Fig 6-A. were identified as living organoids since they were all rounded up and in bubble-form. In Fig 6-B-C-D, organoids were surrounded with dead cells. These cells are likely to present uninfected cells of the original cell cluster that have died during the selection process. Normally, the differentiated dead cells that have completed their task and die via apoptosis are dumped into the lumen of the organoids. In Fig 6-A, organoid already demonstrates the formation of a crypt bud located at the top side of its lumen only 3 days after selection antibiotic puromycin was removed from the media.

Infected mouse intestinal organoids that were able to survive the puromycin selection were grown for another 6 days in regular ENR media with change of media in every 2

days. During these 6 days, most of the intestinal organoids that were infected with a SIRT-1 targeting lentivirus were not able to regenerate new crypts and died. Only 2 out of 76 organoids transduced with B2 lentivirus were able to survive (counted on 9 days post puromycin selection). All other organoids remained in a shape of a single spheroid, indicating that they could not produce new crypts, and died. In contrast, the 2 surviving organoids, which were both infected with Sirt-1 targeting B2 lentivirus, were growing and regenerating new crypt buds as seen in Fig 7.

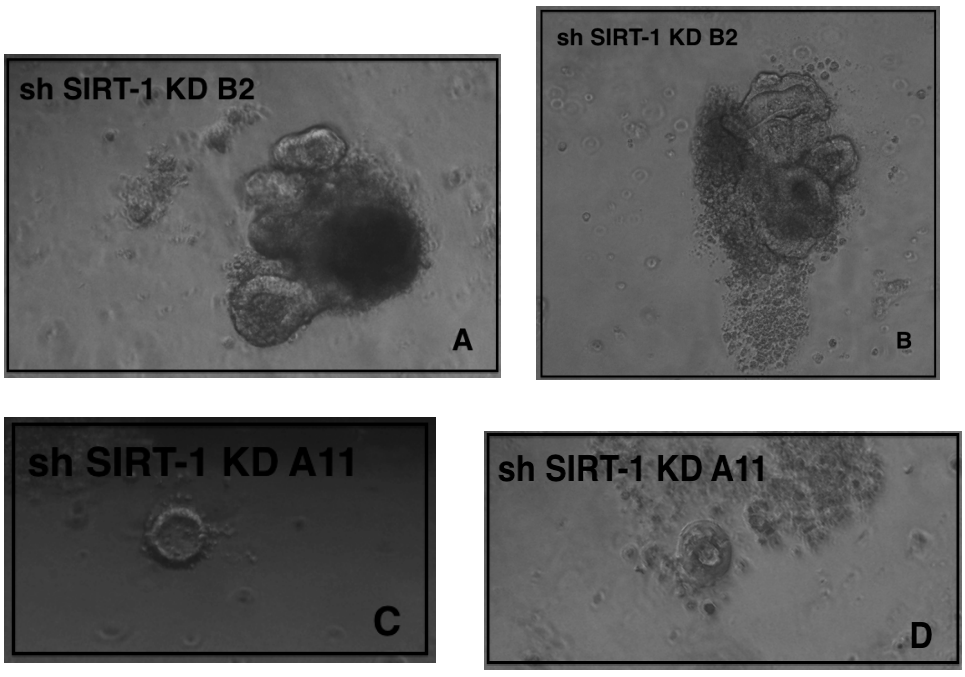

Fig 7. A-B. Only two mouse intestinal organoids transduced with SIRT-1 knocking down B2 lentivirus regenerated multiple crypt domains. All other transduced organoids (both B2 and A11 transduced) were either dead or couldn't regenerate by the time these two organoids were able to regenerate new crypt domains. **C-D.** Clearly showing two organoids, transduced with A11 lentivirus, which were still alive but could not regenerate. All four images were taken at the same day (day 9 post puromycin selection) with 10x objective.

4.7. Activation of Sirt-1 Gene in Mouse Intestinal Organoids

Resveratrol prepared at different concentrations in Regular ENR Media was applied on mouse intestinal organoids grown in vitro embedded in Matrigel for 3 days. Control organoids received regular ENR Media with equal amount of pure ethanol that the resveratrol group received. Fig 8. shows the images of groups of organoids before the addition of ENR media containing resveratrol. Images are all taken from the center of the wells on day 3 of the experiment with 5x objective. Organoids in each well were also counted in order to make sure that all experimental groups were formed by approximately equal number of organoids. Images taken at 5x objective show that crypts had rounded up and formed organoids, and were therefore at a morphologically preferred phase to initiate the experiment. Most of the organoids were just starting to have new crypt buds. In general, organoids were equally viable and at the very early stages of their growth. This was the perfect point to add a new chemical like resveratrol into the organoid media to see how the chemical could affect certain biological characteristics of the organoids such as the number of crypts budding from an organoid, crypt length, crypt width, and Paneth cell count at crypt bottom/tip.

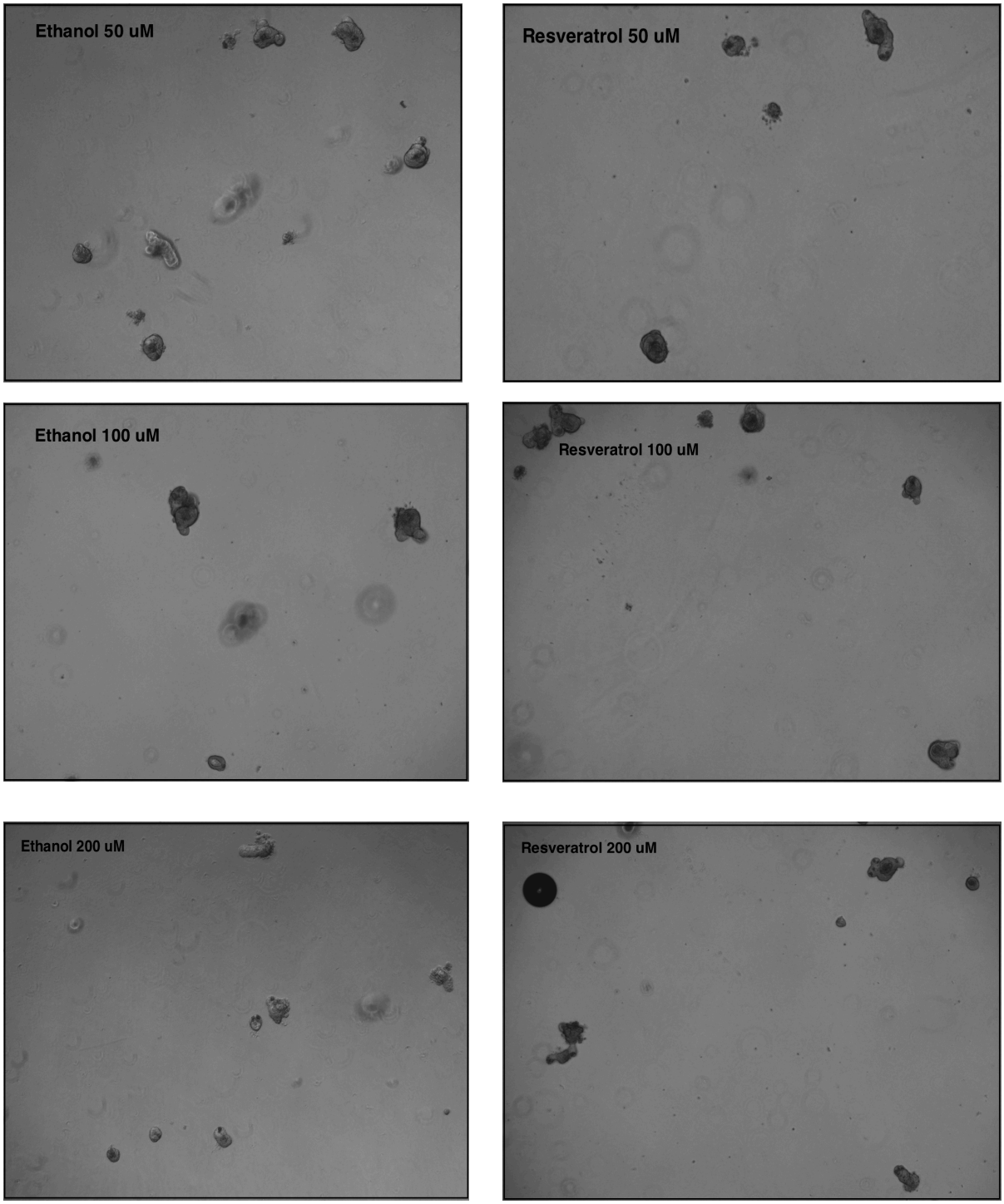

Fig 8. Mouse intestinal organoids before the addition of ENR media with resveratrol. All organoids were equally viable and at the similar stages of their growth phase possessing visibly formed round lumen and few newly budding crypts. Images were captured at 5x objective.

After the organoids were grown in ENR media containing different concentrations of resveratrol, organoids were counted to see if there was any difference in the survival rate between the resveratrol groups and the control groups. Fig 9. shows the number of surviving organoids before the addition of resveratrol as well as 2 days after resveratrol media was added.

	Number of Organoids Surviving at Day 3 (Resveratrol Added)	Number of Organoids Surviving at Day 5
Ethanol-50 µM	24	21
Ethanol-100 µM	28	24
Ethanol-200 µM	25	22
Resveratrol 50 µM	29	23
Resveratrol 100 µM	32	25
Resveratrol 200 µM	27	2

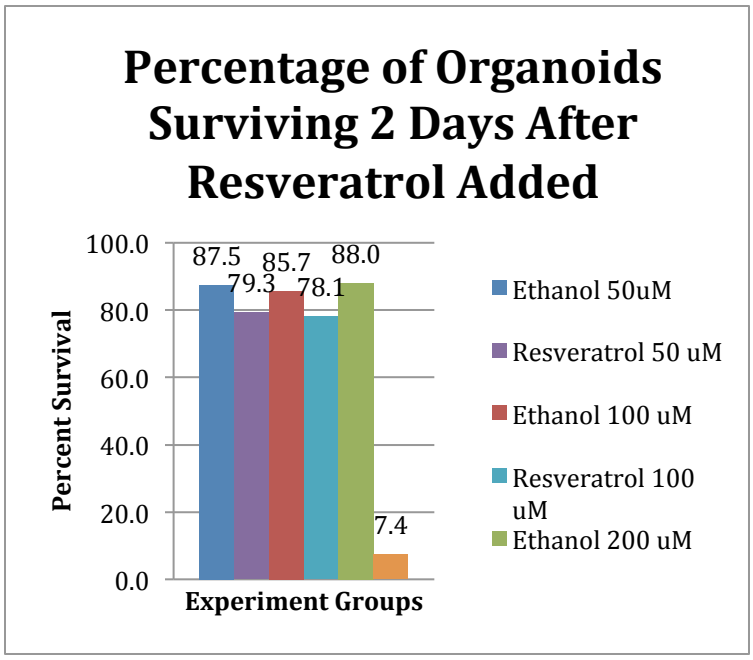

Fig 9. Percent of organoids surviving after two days exposure to resveratrol in ENR media. Organoids, which were grown in ENR media containing 200-µM resveratrol, had the lowest survival rate when compared to its control group receiving equal amount of pure ethanol but no resveratrol.

When the percentage of organoids surviving in each resveratrol receiving group was compared to its corresponding control group, the biggest difference was seen among organoids, which were grown in ENR media containing 200-μM resveratrol and its control group. Even though the experimental groups, which received either 50-μM or 100-μM Resveratrol, had few more organoids dying compared to their control groups, the difference was as low as 7-8%. Organoids, which received equal amount of pure ethanol that the resveratrol 200-μM group received, had survivability rate of 88% whereas the experimental group that received ENR media with 200-μM had only 7.4% of its organoids surviving. In resveratrol 200-μM group, only 2 out of 27 organoids were surviving after they were grown in ENR media with 200-μM resveratrol for 2 days. Two surviving organoids were also different in morphology compared to organoids of the control group; both organoids had only their lumens formed with no crypt budding. On the contrary, control organoids had multiple crypts regenerating from the lumen as seen in Fig 10.

Fig 10. Organoids after 2 days growth in ENR media containing different concentrations of resveratrol. In all groups of organoids except the group, which received ENR media with 200-μM resveratrol, surviving and budding organoids can be observed. It is important to note that the images can be misleading at the first glance because organoids are embedded in a three dimensional matrix and it is not possible to image them all with high definition since they are located at different layers along the z-axis. Dead organoids can be differentiated from living ones by observing the randomly dispersed cells located close to each other, which used to make up a living organoid. *(Images are provided in the next page).*

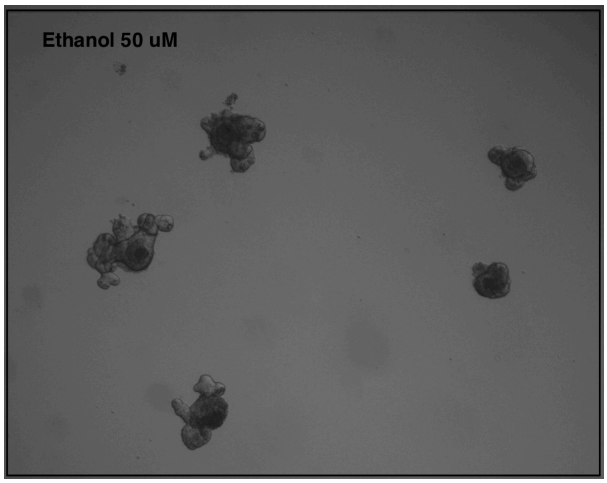
Ethanol 50 uM

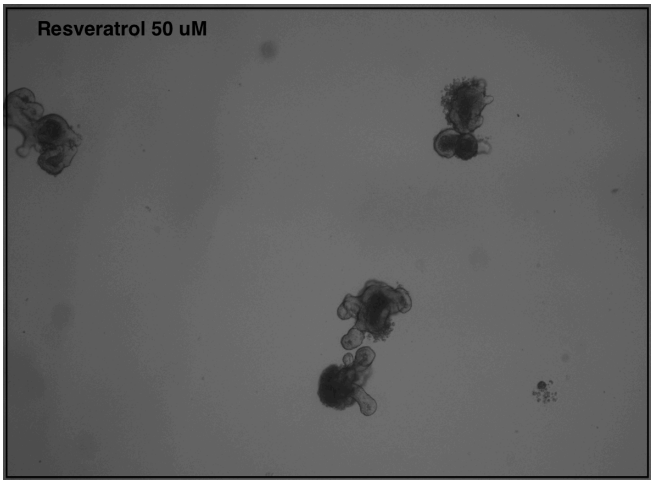
Resveratrol 50 uM

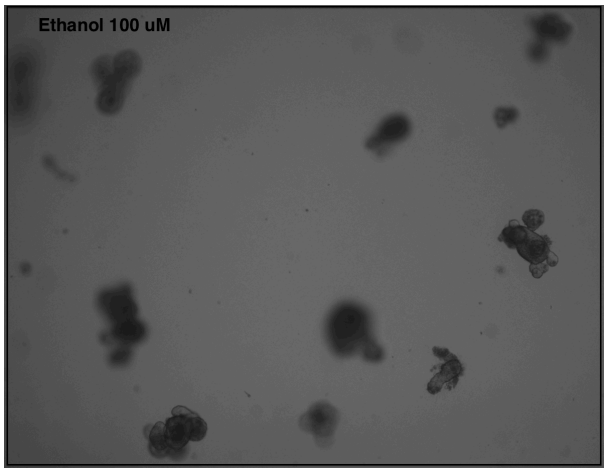
Ethanol 100 uM

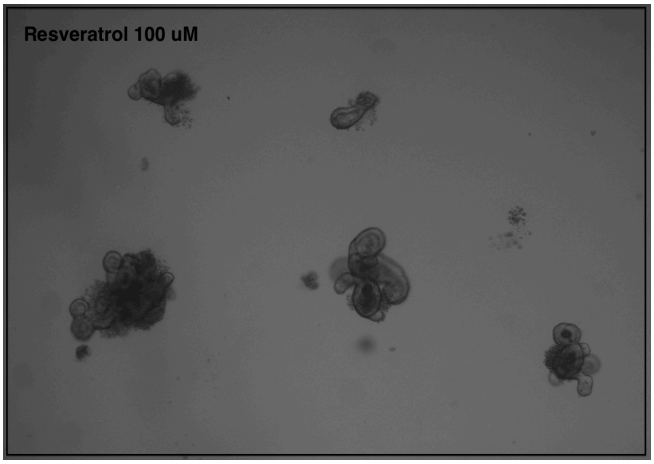
Resveratrol 100 uM

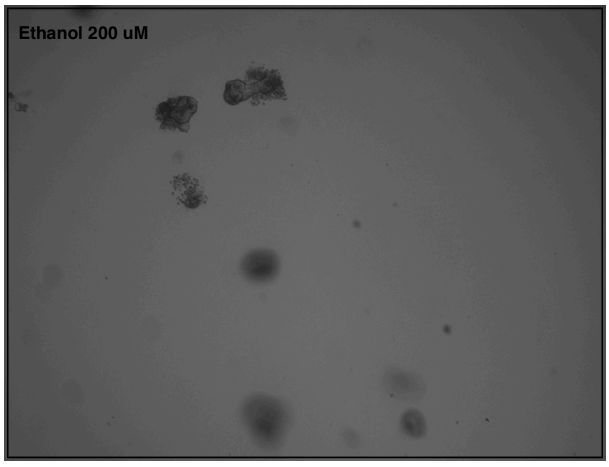
Ethanol 200 uM

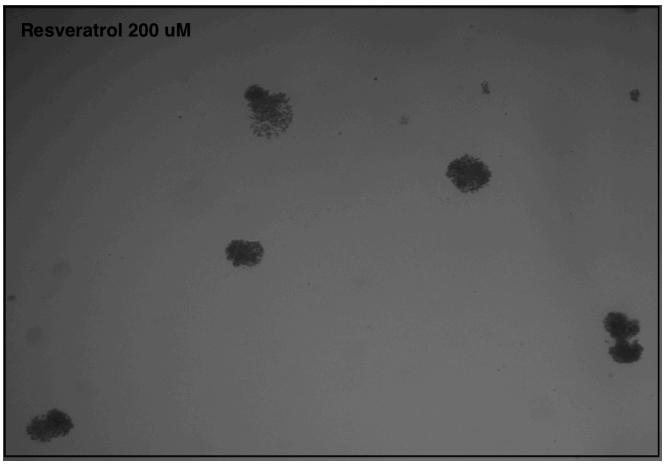
Resveratrol 200 uM

4.8. Effects of Resveratrol on the Regeneration of Intestinal Crypts

In day 6, images of organoids were taken in order to analyze the morphological characteristics of organoids exposed to different concentrations of resveratrol. First, crypts of 13-17 organoids from each experimental and control group were counted and the average crypt number per organoid was calculated. Organoids, which received 200-μM resveratrol, were not included in any of the following analysis since all organoids were dead by day 6. Control organoids that received 200μM of pure ethanol were also omitted from any further analysis. In addition, not all organoids were used in the analysis because some organoids had too many crypts budding from the organoid lumen in all directions in all three planes. So, it was not possible to accurately count these organoids and the decision was to leave them out of the analysis. However, there was almost equal number of organoids that had uncountable number of crypts in each group including the control groups that received no resveratrol, which was an indication that leaving these organoids out of the analysis wouldn't affect the final result. According to the analysis, organoids that received ENR media with resveratrol showed a trend for having fewer crypts per organoid in average compared to the control organoids, which received only ENR media with pure ethanol. Two-tailed T-test analysis was then performed in order to determine if the difference in the average number of crypts per organoid in different experimental groups was statistically significant. According to the P-values shown in Fig 11 difference in the average number of crypts per organoid among different organoid groups was not statistically significant. So, it is possible to conclude that in this one experiment resveratrol had no significant

effect on the average number of crypts per organoid at 50-µM and 100-µM concentrations. However, repeat experiments that would allow statistical comparison of average crypt numbers, not distribution of crypts numbers in a single experiment would be necessary to conclude whether resveratrol has effects on the crypt number. Since all of the organoids that were treated with 200-µM resveratrol in ENR media were dead, we assume that resveratrol in high concentrations can be lethal for intestinal organoids and inhibit the crypt budding completely. However, in lower concentrations, resveratrol had no measured or observed effect on the average number of crypts budding from an intestinal organoid.

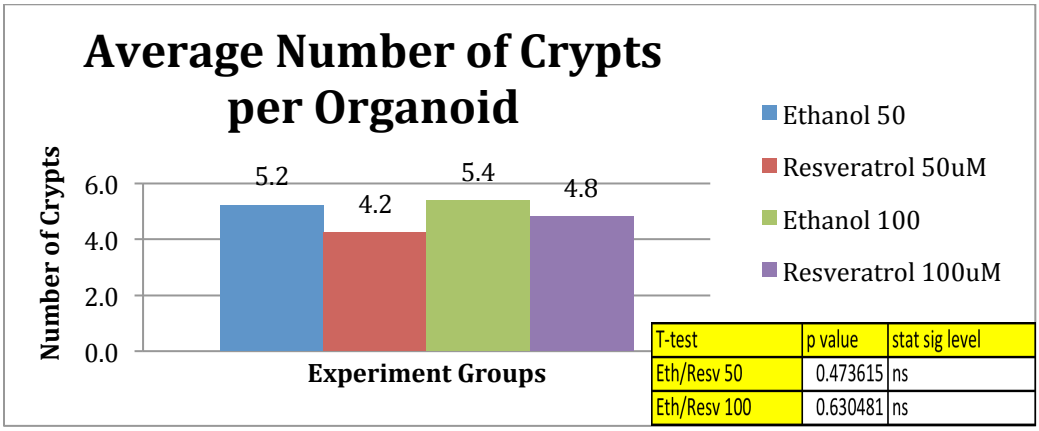

T-test	p value	stat sig level
Eth/Resv 50	0.473615	ns
Eth/Resv 100	0.630481	ns

Fig 11. Average number of crypts of organoids exposed to resveratrol for 2 days. Crypt buds of intestinal organoids treated with a range of resveratrol concentration were counted and the average number of crypts for each experimental and control groups were calculated. Two-tailed T-test was performed and the calculated difference in the average number of crypts per organoid was found to be statistically insignificant as shown above.

4.9. Effect of Resveratrol on Crypt Morphology

4.9.1. Crypt Length

Other morphological characteristics that were at the center of interest were average crypt length and average crypt width. Image J was used in order to measure the crypt length and width and determine if resveratrol had any effect on the size and the length of the regenerating crypts. Crypt lengths were measured from the side of the lumen until the tip of the crypt bud. Crypt widths were measured only at the tip of the crypts, where the crypts were visibly narrowed. According to the results and statistical analysis, it is possible to state that the organoids treated with 50-µM resveratrol in ENR media had shorter crypts compared to the control organoids which received only the same amount of pure ethanol in ENR media. However, difference in average crypt length was not statistically significant in between the organoid group treated with 100-µM resveratrol and its corresponding control group. The statistical insignificance in the result might be caused by the effect of higher volume of ethanol in ENR media on average crypt length. Analysis of the results on average crypt lengths of organoids treated with different concentrations of resveratrol shows that resveratrol in low concentrations (50-µM) have an inhibiting effect on the average length of the crypts whereas it has no further effect on average crypt length if the resveratrol concentration was doubled (100-µM). However, also the organoids treated with 100µM resveratrol trend towards having shorter crypts than their control counterparts.

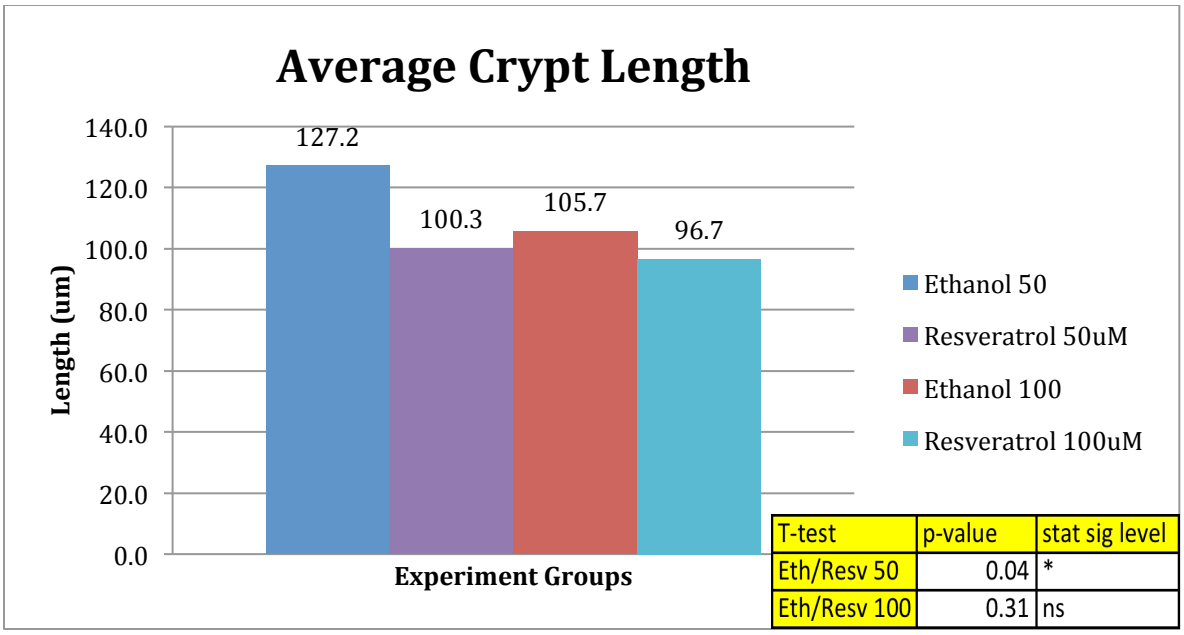

T-test	p-value	stat sig level
Eth/Resv 50	0.04	*
Eth/Resv 100	0.31	ns

Fig 12. Average crypt length of organoids treated with resveratrol for 2 days. Crypt lengths of intestinal organoids treated with different concentrations of resveratrol were measured by using Image J and the average length for experimental and control groups were calculated. Two-tailed T-testing was done to show the significance level of the differences in average crypt lengths of organoids between experimental and control groups.

4.9.2. Crypt Width

Width of regenerating intestinal crypt buddings were measured and analyzed to determine if resveratrol in ENR media had an effect on the size of the crypt buddings. Only crypts that were growing perpendicular to the z-axis were included in the analysis in order to accurately measure the crypt widths. Around 11-13 crypts from each group meeting the criteria for inclusion in analysis were measured and the average size of crypt widths were calculated. Two-tailed T-test was used to see if the differences in average measurements were statistically significant. Organoids grown in ENR media containing 50-µM resveratrol had in average crypt widths in the size of 36.8-µm

whereas the control organoids that were exposed to same amount of pure ethanol had in average larger width at the crypt bottom in the size of 52.0-µm. Organoids that were treated with 100-µM resveratrol in ENR media had also smaller crypt widths compared to the control organoids, crypt width in average differing by 11.7-µm. Average crypt widths as well as the statistical significance of the results for all organoid groups are given in Fig 13. Results show that resveratrol in ENR media has an inhibiting effect on the growth of crypt width at the crypt bottom.

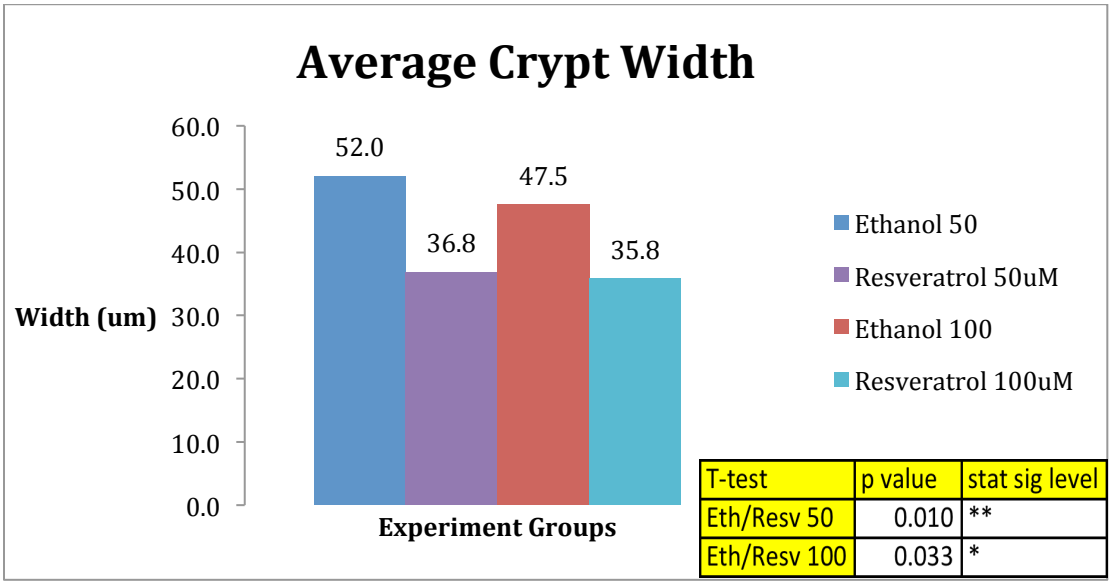

T-test	p value	stat sig level
Eth/Resv 50	0.010	**
Eth/Resv 100	0.033	*

Fig 13. Average crypt width of organoids grown in resveratrol containing media for 2 days. Crypt width of organoids treated with different concentrations of resveratrol in ENR media were measured in Image J and the average values shown above were calculated. Two-tailed T-test was used to determine the p values and the statistical significance of the results. Analysis shows that application of resveratrol on organoids reduced the regenerating crypt bottom widths at a statistically significant level.

4.10. Effect of Resveratrol on Paneth Cell Count in the Crypt Bottoms of Intestinal Organoids

Paneth cells residing at the bottom of the crypts in intestinal organoids were imaged and counted under microscope according to their granularity and shape (See Figure 15). Fig 14. shows the average number of Paneth cells counted under the light microscope at 40x. 10 crypts from each organoid group meeting the similar inclusion criteria that was set for crypt length and width measurements were imaged for their Paneth cells and the visible Paneth cells were also counted. In average, Paneth cell number per crypt bud was measured to be much higher in the control groups than the resveratrol receiving groups. In the organoid group grown in 50-μM resveratrol, average Paneth cell number was 0.7; highest number of Paneth cell counted in a crypt bottom was 2 and the lowest was 0. On the other hand, the corresponding control group of resveratrol 50-μM had in average 4.7 Paneth cells per crypt bud; highest number counted was 12, and lowest was 2. However, difference in Paneth cell count between the organoid group treated with 100-μM resveratrol in ENR media and its control group was larger. Strikingly, there were no Paneth cells visible when imaged under light microscope at 40x objective in resveratrol 100-μM group, whereas its control group had organoid crypt bottoms possessing in average 3.1 Paneth cells (see Fig 14).

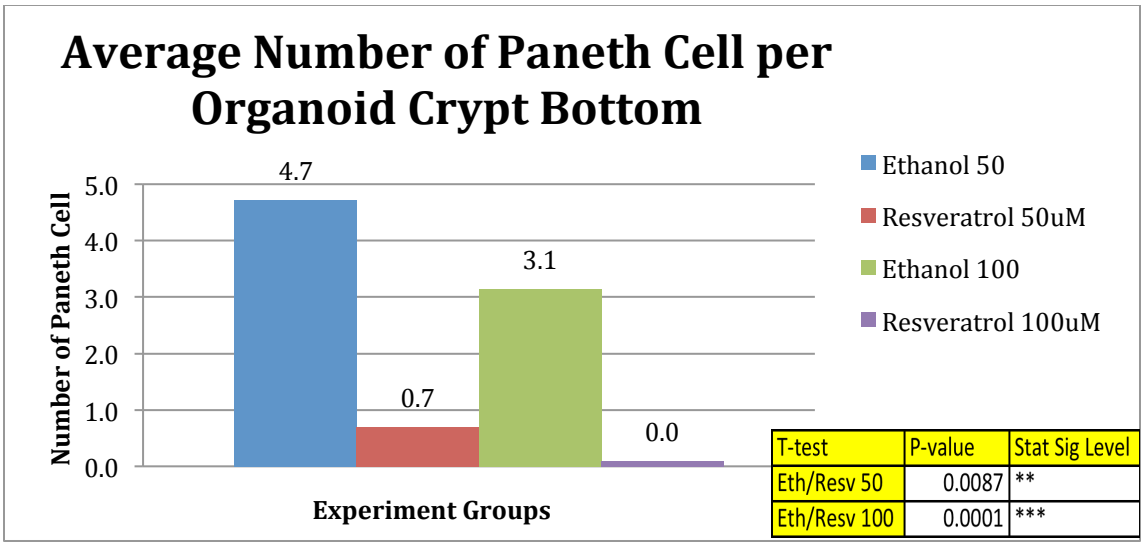

Fig 14. Average number of Paneth cells in crypt tips of organoids cultured in resveratrol containing media for 2 days. Effect of resveratrol on Paneth cell count in the crypt bottoms of intestinal organoids was determined by counting Paneth cells under the microscope with 40x objective. Average number of Paneth cells in experimental and control groups were calculated. Two-tailed T-test was used to determine the statistical significance of the results. Analysis showed that treating organoids with resveratrol of 50-µM or 100-µM in ENR media greatly reduced the number of Paneth cells located in a crypt bottom.

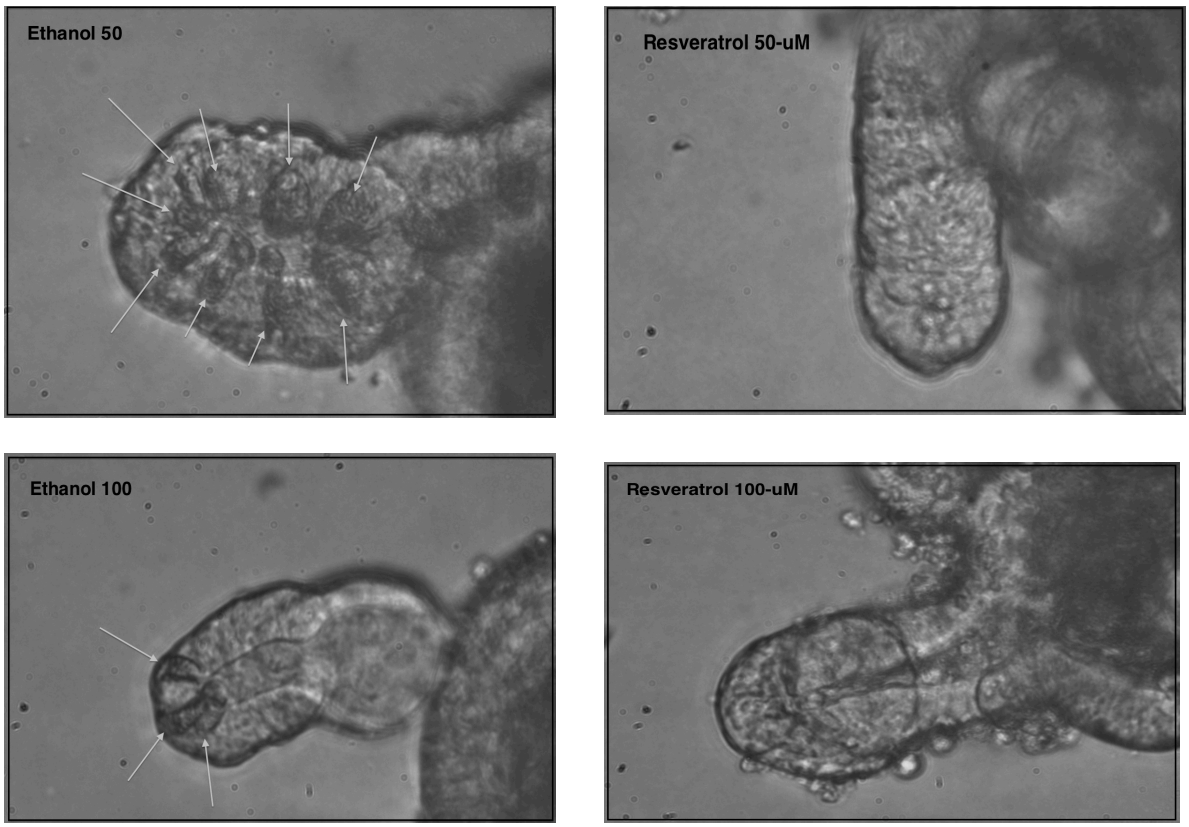

Fig 15. Paneth cells located at the crypt tips/bottoms of resveratrol treated and non-treated intestinal organoids. Crypt buds were imaged at 20x for Paneth cells located in the crypt bottoms. Arrows pointing at the Paneth cells show that control organoids had visible Paneth cells residing at the crypt bottoms. However, organoids which were treated with either 50-µM or 100-µM resveratrol in ENR media had no Paneth cells located in the crypt bottoms as shown in the pictures above.

5. Discussion

5.1. Knocking Down Sirt-1 in Mouse Intestinal Organoids

5.1.1. Analysis of Lentiviral Knockdown Efficiency in NIH 3T3 Mouse Fibroblasts

Transducing wild-type organoids is a very novel technique, optimized in Katajisto Lab only in August 2014, and partly as a part of this thesis work. Therefore, produced lentiviruses were first tested on NIH 3T3 Mouse Fibroblasts. Without successful transduction of NIH 3T3s it would not have been reasonable to advance into intestinal organoid transduction, since the latter is so much harder, tending to exhibit very low transduction efficiencies.

According to the results obtained from Western Blotting and Image J Analysis, protein lysates obtained from lysed NIH 3T3 shRNA- B2 cells and NIH 3T3 shRNA- A11 cells contained very low amounts of SIRT1 protein when compared with the analyzed lysate of control cells transduced with non-targeting non-SIRT1 specific lentivirus.

Upon discussion with my supervisor, I decided to continue my intestinal organoid transductions with lentiviruses named B2 and A11. Lentivirus B3 was not chosen as a candidate for further experiments since it displayed a lower SIRT1 knockdown efficiency compared to other two lentiviruses.

Advancing to the next stage with B2 and A11 had both its advantages and disadvantages. Since both lentiviruses exhibited very high knockdown efficiency in the target gene, especially lentivirus A11 knocking down SIRT1 almost by 98%, it was expected, that we would observe close to maximal phenotypic alterations on the

organoids and the regeneration rate of the crypts. Even though high knockdown efficiencies of these viruses might be considered as an advantage, this could also become a disadvantage as the high knockdown of a gene like SIRT1, which contributes to cellular proliferation and apoptosis, could actually be lethal for the intestinal organoids. Such an outcome would inhibit us from studying the role of SIRT1 in crypt regeneration rate, and its impact on crypt length and width as well as Paneth cell count located in crypt tips.

5.1.2. Possible Effect of Sirt-1 Knock Down on Intestinal Organoid Size

After intestinal organoids were transduced with chosen lentiviruses, puromycin selection method was used to identify the organoids, which were actually transduced. In the day of transduction, organoids were disintegrated into single cells or cell clusters. After this disintegration process, Lgr5+ intestinal stem cells can be found as single cells or part of cell clusters. To prevent the spontaneous differentiation of stem cells in vitro, CHIR compound and Valproic Acid were utilized to trick stem cells into thinking they were in physical contact with Paneth cells by stimulating Wnt and Notch signaling pathways. Managing to infect a single stem cell with a SIRT1 targeting lentivirus would provide us intestinal organoids with cells all containing the viral gene in their genome as a single stem gives rise to a full grown intestinal organoid.

Two-days post transduction of disintegrated intestinal organoids, there were organoids growing in all four experimental groups (no virus, non-targeting, B2, and A11). An interesting difference observed between the organoids belonging to different groups was that the organoids with one of the two SIRT1 knocking down lentiviruses were

bigger in size compared to the organoids which were presumably transduced with non-targeting virus or no virus. However, it was not yet proven if these organoids were actually transduced since the selection antibiotic puromycin was not yet applied.

In previous research, conflicting results were reported on the ability of SIRT1 to promote or inhibit cell proliferation and apoptosis in intestinal epithelium. According to a study that was done with mouse intestinal epithelium in normal physiological conditions, global knock out of SIRT1 in mice promoted intestinal cell proliferation and suppressed cell apoptosis in the gut.[101] Along the same lines, organoids, which were presumably transduced with knockdown lentiviruses, were much bigger in lumen size compared to the control organoids. However, the significance of this observation is hard to judge, as it manifested prior to puromycin selection of infected organoids, and because organoids transduced with non-targeting virus died during the selection. In case the intestinal organoids larger in lumen size would have demonstrated better survival than organoids with smaller lumen, this would have meant that the difference in lumen size was likely due to lentiviral knockdown of SIRT1. However, there was no trend observed between the organoid lumen size and survivability after puromycin addition as small and larger organoids were killed with similar frequencies by puromycin.

5.1.3. Selection of Successfully Transduced Mouse Intestinal Organoids

After organoids went through the transduction procedure, puromycin selection was used to select the successfully transduced organoids and eliminate the non-transduced ones. Organoids, which were not transduced, were all killed due to the puromycin effect

as expected. Organoids, which were transduced with B2 and A11 knockdown viruses, had survivability rates of 24% and 12%, respectively. However, organoids, which were transduced with the non-targeting non-Sirt1 specific control lentiviruses, were all killed upon applying puromycin, showing that the transduction of organoids with the control virus was not successful. As the same non-targeting control virus was successfully used in the set-up experimentes with NIH-3T3, and presented similar infectivity as the B2 and A11 viruses, it is unclear why organoids were not infected with the control virus. The experiment was conducted only once (see below) so any error in the transduction protocol, or during selection could count for this. Also, as only 12-24% of organoids survived with A11 and B2 viruses, there was only a small window for infection by non-targeting control to be detected, if it showed any lower transduction frequency.

This situation left me with no control organoids surviving after puromycin selection but only organoids, which were transduced with SIRT1 knockdown lentiviruses. It was an option to quit the experiment to start over and redo it but I chose to continue with the experiment. The experiment couldn't also be redone quickly since there was no more control viruses left in the stock. I would need to prepare more control viruses together with knockdown viruses, since all viruses have to come from the same batch when doing a comparison study. I would also need to infect another set of NIH 3T3 cells with these new viruses, select the transduced ones, grow them, and perform another Western Blot and Image J Analysis to determine the Sirt1 knockdown efficiency of these new viruses. This would be followed by an isolation of a new small intestine from a mouse and culturing the organoids in vitro for a week before the transduction could

take place with no guarantee that the transduction would work perfectly this time since the protocol was very new and required more optimization to achieve higher transduction efficiencies. In short, in order not to repeat the work done in the past 1.5-2 months, I decided to continue with my experiment and analyze the effect of Sirt1 knockdown on my organoids without the control organoids, which could be considered as a shortcoming of this experiment.

5.1.4. Effect of Sirt-1 Knock Down on Mouse Intestinal Organoid Maintenance

Successfully selected mouse intestinal organoids were cultured for another 9 days after the selection was complete. Even though the organoids were able to survive the selection, which indicated that they were successfully transduced, almost all of them either could not regenerate new crypt buddings or couldn't regenerate and died in their lumen form. Organoids transduced with the A11 lentivirus that knocked down SIRT1 by 98% were all dead or in lumen form 13 days after transduction (9 days after puromycin selection was complete). Organoids transduced with the B2 lentivirus that knocked down SIRT1 by 88% were almost all dead too, only 2 organoids surviving and regenerating new crypt buds. As I did not have the proper control (transduced with a non-targeting virus) organoids, I can only compare the A11 and B2 transduced organoids to organoids that have not been transduced at all. Such un-transduced organoids can be grown quickly to form miniguts that contain multiple crypt domains (see for example Figure 10) and show no tendency to die over a short 9-day culture.

The reason why transduced intestinal stem cells were able to form short-term organoids but not regenerate crypt buds may be complex as SIRT1 was attributed to

contradicting roles as either tumor-promoting/cell proliferative or tumor-suppressor/cell proliferation inhibitor. However, an explanation to this result might be as follows: intestinal stem cells with SIRT1 knockdown were able to form organoids and luminal structures because they were supplemented with Wnt ligand. Normally organoids do not need additional Wnt ligands as stem cells receive wnt –signals from the Paneth cells, but when organoids are dissociated, and Paneth-ISC contacts are lost, cultures must be supplemented with Wnt3A for a period of 1-2 days. Wnt ligand stimulated the Wnt signaling pathway and promoted cell proliferation and the formation of the organoids. The organoids were not dying because the presence of β-catenin, a downstream effector of Wnt signaling pathway, was promoting the self-renewal of intestinal stem cells after they were dividing and giving rise to a stem cell and a differentiated cell. β-catenin can mediate the activation of Wnt target genes, promoting cell proliferation of the crypt epithelium. However, after organoids were selected with puromycin Wnt ligand was no more included in the organoid culture media in order to see the full and unique effect of SIRT1 on mouse intestinal organoid maintenance.

SIRT1 is also a stimulator of Wnt signaling pathway and in the absence of Wnt ligand and SIRT1 stimulation, intracellular β-catenin levels might be steeply reduced and caused the differentiation of the stem cells into mature cells of intestinal epithelium. Inhibition of SIRT1 was previously shown to inactivate β-catenin in colorectal carcinoma cells. When there was no stem cell left to give rise to healthy differentiated

cells due to the stem cells' quick differentiation caused by very low β-catenin levels arising from lack of Wnt and Sirt1 signaling, organoids started to die.

Now the question is how can the two organoids manage to overcome SIRT1 knockdown effect and regenerate crypt buddings even when Wnt ligands were removed? Surprisingly, the two organoids, which were able to survive and regenerate new crypts, had already been started to give rise to new buds in the presence of Wnt ligand. So, it is possible, that when Wnt ligand was no longer provided in the culture media, crypts managed to continue to further grow due to Wnt ligands produced by Paneth cells of the crypts and organoids were not killed by the severe SIRT1 knockdown. However, the actual reason why these two organoids transduced with B2 lentivirus were able to regenerate crypts and do this faster than other organoids cannot be fully explained with the experimental results in hand. One reason might be that these two organoids might have managed to mitigate the effect of the viral knockdown on their survivability by successfully silencing the virally integrated gene on their genome. Puromycin could have been reused again to see if all of the cells of these two organoids were still resistant to the selection marker. However, this was not thought on the right time by me and was not essayed.

98% inactivation of SIRT1 in mouse intestinal organoids might also have interfered with IIS signaling pathway, preventing the proliferation of intestinal epithelial cells and the regeneration of new crypt buddings. It has been previously shown that mice with global SIRT1 deletion express severe growth retardation and reduced blood levels of

free IGF-I.[99] Severe reduction in SIRT1 expression levels might have also severely reduced the functioning of IIS signaling pathways, leading to the death of the organoids. Even though reducing IIS signaling was previously shown as a defensive mechanism against aging[36-37], extremely low expression levels of the genes belonging to this pathway was shown to be lethal to organisms as it will greatly inhibit cellular proliferation and healthy functioning of the metabolism.[38-39]

Another reason why SIRT1 knockdown intestinal organoids could not regenerate and die only after forming the luminal structure might be related to reductions in AMPK signaling pathway. AMPK plays significant role in improving lifespan by regulating energy homeostasis, stress resistance, and cellular housekeeping.[45] AMPK was also shown to prolong lifespan in lower organisms when upregulated.[45] SIRT1 is known to engage in a positive feedback loop of activation with AMPK, higher SIRT1 levels more AMPK will be activated.[47] In mouse intestinal organoid models with effective SIRT1 knockdown, the activation signaling from SIRT1 on AMPK might have disappeared. Very often aging is accompanied by reductions in AMPK signaling.[46] Thus; knockdown of SIRT1 might have reduced AMPK signaling and speeded up the aging of intestinal organoids, causing them to die before they could regenerate new crypts.

5.2. Activating Sirt-1 in Mouse Intestinal Organoids By Applying Resveratrol

5.2.1. Impact of Resveratrol on Mouse Intestinal Organoid Survivability

Resveratrol is a candidate drug for treating aging-associated diseases, especially Type-2 diabetes. Activation of SIRT1 by resveratrol may be used as a treatment method in the

future to ameliorate the healthspan of aging populations, which will be very likely to suffer from a variety of aging-associated diseases including Type-2 diabetes, obesity, cardiovascular diseases, and cancer.

In this study, we wanted to observe the role of SIRT1 in mouse intestinal organoid maintenance. More specifically, we were interested in if SIRT1 could alter intestinal crypt regeneration by regulating the proliferation and apoptosis of intestinal stem cells and Paneth cells.

Applying different concentrations of resveratrol to fully functional and viable intestinal organoids displayed a possible negative effect of resveratrol on organoid viability and regeneration. Organoids, which were treated with highest concentration of resveratrol (200-µM) in the experimental design, exhibited the lowest survival rate of only around 7%, which is 81% lower than the survivability rate of the control group. In concordance, while SIRT1 can be targeted for activation to prevent the development of aging-associated diseases, to enhance energy balance, and to regulate cell proliferation and apoptosis in many organisms, activating SIRT1 high above it physiological levels was previously shown as lethal.[101-102]

5.2.2. Resveratrol Effect on Crypt Regeneration

Several metric were analyzed to determine if resveratrol affects crypt regeneration. First, we examined the effect of resveratrol on average number of crypts forming per organoid to determine if resveratrol, by activating its target gene SIRT1, can enhance or inhibit crypt regeneration. Despite the experimental groups, which received either 50-

μM or 100-μM resveratrol in regular organoid culture media, possessed fewer crypts regenerating from organoid lumen compared to the control organoids, the difference was not found to be statistically significant. Thus, we concluded that SIRT1 does not have a role in the number of crypts regenerating from an organoid.

Next, we measured the average crypt length together with average crypt width. Resveratrol treated groups were found to have shorter crypts compared to controls. At 50-μM resveratrol was able to slow down the regeneration rate at a level of statistical significance, whereas at 100-μM the difference in crypt length was not statistically significant between resveratrol treated group and the control group. Shorter crypts typically indicate slower rate of proliferation by the two proliferative cell types of intestinal crypts: the ISCs and transiently amplifying cells. We did not address which type of cell was responsible for the reduced crypt length, but reduced proliferation by either cell type will also result in reduced regeneration, and could also explain the (non-significant) trend towards fewer crypts.

Finally, applying resveratrol to mouse intestinal organoids affected the width of the regenerating crypts at a great extent and statistically significant. Resveratrol treated organoids possessed narrower crypts compared to the controls at a level of statistical significance. Surprisingly, the difference was relatively bigger between organoids treated with 50-μM resveratrol and its controls compared to the difference in crypt width between the organoids treated with 100-μM resveratrol and its corresponding controls. Similar trends were seen with other used crypt measurements. We can not

conclude whether this is due to SIRT1 activation having maximal effects at 50μM or due to the higher concentration of ethanol masking effects with 100μM concentrations.

5.2.3. Effect of Sirt1 Activation on Paneth Cell Proliferation

We demonstrated that Sirt1 activation by resveratrol to very high levels was lethal for mouse intestinal organoids. Sirt1 activation also displayed growth-inhibiting effect on regenerating crypts, leading to shorter and narrower crypts compared to controls. To get a better insight on why these crypts were narrower and also growing slower, we wanted to analyze the Paneth cell composition of crypt tips of intestinal organoids. Intestinal stem cells (ISCs) reside at the crypt bottoms/tips in the single cell layered intestinal epithelium. ISCs are in direct physical contact with two Paneth cells on both sides, which signal them to stay in the stem cell state and enable their self-renewal ability. When stem cells lose contact with Paneth cells, they spontaneously differentiate into other cell types of intestinal epithelium.

Paneth cells can easily be distinguished from other cell types by their granular structure under the light microscope with 40x objective. Since ISCs are found in the middle of two Paneth cells, counting Paneth cells can give us an approximate result on the number of ISCs located in a given crypt tip. Additionally, growth of an intestinal crypt is driven by the cycles of proliferation and differentiation of intestinal stem cells. Possessing more stem cells can be considered beneficial in the beginning; however, it can also lead to a fate of faster growth and a quicker death for the organoids if these stem cells are actively proliferating and differentiating. Therefore, it might actually be more beneficial

for an organoid to possess less but more dormant stem cells in order to extend its lifespan.

My observation of Paneth cell numbers, and thus the number of stem cells, in a crypt tip can explain the slower growth in length and width in mouse intestinal organoids treated with resveratrol. We hypothesized that we would observe less Paneth cells in crypt tips of organoids treated with resveratrol since they exhibited narrower crypt tips compared to the control organoids. According to the observations, our hypothesis was right. Indeed, organoids that were treated with 50-μM resveratrol had an average of 0.7 Paneth cell per organoid tip, some crypt tips exhibiting no Paneth cell at all. Doubling resveratrol concentration to 100-μM reduced the visible Paneth cell number to 0. On the contrary, the control organoids for 50-μM and 100-μM resveratrol had in average 4.7 and 3.1 Paneth cells, respectively. Therefore, we conclude that Sirt1, activated by resveratrol, controls the differentiation Paneth cells in mouse intestinal crypts, and therefore influences the number of stem cells that are dependent on contacts with Paneth cells. Reduced number of Paneth cells may also explain the reduced crypt width as Paneth cells are large.

Even though almost no Paneth cell was observed in crypt tips of organoids treated with 100-μM resveratrol, we believe that there were actually some Paneth cells, or cells with Paneth cell-like stem cell supporting activity, but that they were thinner and smaller compared to the normal size of a Paneth cell. Otherwise, there would not be any intestinal stem cell existing in these crypt tips, leading to the death of the organoid. That is actually what we think that happened in organoids that were treated with 200-μM resveratrol; overexpression of Sirt1 mediated through resveratrol inhibited Paneth cell

differentiation to an extent that there were no Paneth cells to create the niche required for stem cells to be able to self-renew themselves. Furthermore, low Paneth cell number would lead to the differentiation of the accompanying stem cells and would eventually cause the death of organoids. In parallel to our findings, and while this thesis work was on-going, Sirt1 was also found to be a regulator of Paneth cell number in crypt tips of intestinal epithelium.[106] Mice with an intestinal specific Sirt1 deficiency were found to possess more Paneth cells compared to controls.[106] However, I did not observe high increases in Paneth cell number in crypt tips of Sirt1 knockdown organoids. Reason might be that the knockdown on the in vitro organoid cultures occurs without the native interactions between intestinal epithelium and mesenchymal cells, and that loss of Sirt1 in this context may result in organoid death even if loss of Sirt1 in vivo can be compensated and results only in overrepresentation of the secretory lineage cells. On the other hand, the findings by La Sasso et al.[106] are perfectly in line with my findings on the dramatic reduction of Paneth cell number with SIRT1 activation by Resveratrol. It will be interesting to address if the reduced number of Paneth cells due to SIRT1 activation, that I discovered, could also indicate that Resveratrol reduces the number of cycling Lgr5+ stem cells, and could therefore have strong effects on intestinal homeostasis and for example tumor incidence.

Intestinal organoids that were treated with 100-μM resveratrol had much less Paneth cells, and thus stem cells, compared to the control organoids. Consistently, organoids treated with 100-μM resveratrol exhibited a slower rate of crypt regeneration, possessing shorter and narrower crypts compared to controls. However, the remaining stem cells in resveratrol treated groups (except 200 μM) were still able to support

proliferation and differentiation and enable the organoid to grow and regenerate new crypt buddings. Surprisingly even the complete lack of observed Paneth cells in 100μM treated organoids did not result in significant reduction in crypt numbers per organoid. However, repeat experiments are necessary, as also crypt number was showing a trend for lower values.

5.3. Concluding Remarks on Thesis Results

In this project, we essayed to identify the role of Sirt1, an NAD^+-dependent deacetylase known to regulate vital cellular mechanisms such as proliferation and apoptosis, energy balance, and glucose and lipid metabolism, in the maintenance of mouse intestinal organoid models. We investigated the role of Sirt1 by taking two different approaches. First, we knocked down Sirt1 gene in mouse intestinal organoid models by transducing the organoids with lentiviruses. Later, we performed drug-mediated activation of Sirt1 by utilizing commercially available resveratrol. In both approaches, we observed how the inhibition or the activation of Sirt1 would affect mouse intestinal organoid maintenance and whether the organoid model would benefit from overexpression and/or deactivation of Sirt1 gene. More specifically, we were interested in how activation and deactivation of Sirt1 would alter the regeneration of intestinal crypts and their growth rate. To understand the results we observed, we tried to make a connection between the Paneth cell and intestinal stem cell composition of intestinal crypt tips with the rate of regeneration and the size and number of regenerated intestinal crypts.

We demonstrated that severe knockdown of Sirt1 gene inhibited the regeneration of new intestinal crypt buddings and caused the death of the intestinal organoids. Severe

deactivation of Sirt1 might have reduced the activity of complex signaling pathways such as Wnt signaling, IIS signaling, and AMPK signaling pathways, which possess significant roles in regulating many different metabolic activities. Moreover, activating Sirt1 much above its physiological levels also exhibited lethal impact on intestinal organoids. We showed that activating Sirt1 with resveratrol slowed down the regeneration rate of intestinal organoids, leading to the formation of organoids with crypts of shorter and narrower in size compared to controls. We also demonstrated that Sirt1 was able to slow down regeneration by controlling the proliferation of Paneth cells located in intestinal crypt tips. Activating Sirt1 reduced the number of Paneth cells located in the crypts of intestinal organoids. Since Paneth cell number in a crypt is positively correlated with stem cell number we can also claim that Sirt1 activation reduced the number of intestinal stem cell in a crypt tip. Activation of Sirt1 to very high levels phenocopied gene-loss-of function that we observed in the knockdown model, by completely inhibiting the formation of Paneth cells and destroying the niche required for stem cells to self-renew in intestinal crypts and leading to the death of the mouse intestinal organoids. In conclusion, severe knockdown of Sirt1 gene through shRNA lentivirus method and very high activation of Sirt1 by resveratrol exhibited similar lethal effects on mouse intestinal organoids; whereas, relatively lower overexpression of Sirt1 via resveratrol exhibited results that deserve to be further investigated in the context of intestinal epithelium dynamics. Relatively low level of activation of Sirt1 slowed down the rate of regeneration by regulating the proliferation of Paneth cells in crypt tips of mouse intestinal organoids.

5.4. Future Prospects

The role of the Sirtuin-1 gene in maintaining mouse intestinal epithelium through its regulatory impact on Paneth cell proliferation and stem cell self-renewal could be investigated in more detail with further experimentation. For example, $Lgr5^{+}$-green fluorescent protein expressing intestinal stem cells with Sirt-1 knockdown can be isolated from other cells through FACS sorting. Knockdown intestinal stem cells can later be cultured with knockdown Paneth cells or normal Paneth cells. This experiment can demonstrate the importance of Sirt-1 activity in Paneth cells in regulating the formation of organoids and self-renewal of the stem cells.

Another possible future experiment can be isolating crypts from mice grown on a calorie-restricted diet. Organoids that transform from these crypts can be compared with organoids transforming from crypts of mice grown on a regular diet. We know that calorie restriction activates Sirt-1 and promotes its beneficial effects on healthspan of rodents. With this way, significance of Sirt-1 activity in maintaining functionally and structurally healthy intestinal organoids can be further demonstrated.

6. Acknowledgements

This project was carried out under the supervision of Pekka Katajisto in the Institute of Biotechnology at the University of Helsinki. First of all, I would like to thank Pekka Katajisto for giving me the opportunity to conduct my thesis project in his laboratory. He always encouraged me to be successful throughout this journey and together with his guidance I was able to complete my thesis project.

I would like to thank Sharif Iqbal for training me and teaching me all the necessary techniques I needed to learn to perform the experiments. I was very lucky to have him teach and guide me. He always answered my endless questions with complete patience and offered me help whenever things did not go so well.

I also would like to thank my fellow team members Julia Döhla, Johanna Englund, Maija Simula, Nalle Pentinmikko, Eino Markelin, Emmi Tiilikainen, and Ella Salminen for always being very positive, friendly, and welcoming to me throughout my laboratory experience. It was a pleasure to work with them all.

Finally, I would like to thank my parents, Ayfer and Erhan Cansu, and my sister, Buket Cansu, for always believing in me. I would neither be able to finish this project nor even study in Helsinki if it wasn't for their complete support and encouragement.

7. References

1. Lopez-Otin, Carlos et al. (2013). The Hallmarks of Aging. Cell *153*.

2. Burtner, C.R., and Kennedy, B.K. (2010). Progeria syndromes and ageing: what is the connection? Nat.Rev. Mol. Cell Biol. *11*, 567-578.

3. Moskalev, A.A. et. al. (2012). The role of DNA damage and repair in aging through the prism of Koch-like criteria. Ageing Res. Rev.

4. Faggioli, F. et al. (2012). Chromosome-specific accumulation of aneuploidy in the aging mouse brain. Hum. Mol. Genet. *21*, 5246-5253.

5. Forsberg, L.A. et al. (2012). Age-related somatic structural changes in the nuclear genome of human blood cells. Am J. Hum. Genet. *90*, 217-228.

6. Gregg, S.Q. et al. (2012). A mouse model of accelerated liver aging caused by a defect in DNA repair. Hepatology *55*, 609-621.

7. Hoeijmakers, J.H. (2009) DNA damage, aging, and cancer. N. Engl. J. Med. *361*, 1475-1485.

8. Park, C.B., and Larsson, N.G. (2011). Mitochondrial DNA mutations in disease and aging. J Cell Biol. *193*, 809-818.

9. Kujoth, G.C. et al. (2005). Mitochondrial DNA mutations, oxidative stress, and apoptosis in mammalian aging. Science *309*, 481-484.

10. Greer, E.L. et. al. (2010). Members of the H3K4 trimethylation complex regulate lifespan in a germline-dependent manner in C. elegans. Nature *466*, 383-387.

11. Siebold, A.P. et al. (2010). Polycomb repressive complex 2 and Trithorax modulate Drosophilia. Aging Cell *10*, 735-748.

12. Jin, C. et al. (2011). Histone demethylases UTX-1 regulates C. elegans life span by targeting the insulin/IGF-1 signaling pathway. Cell Metab. *14*, 161-172.

13. Kaeberlein, M. et al. (1999). The SIR2/3/4 complex and SIR2 alone promote longevity in Saccharomyces cerevisiae by two different mechanisms. Genes Dev. *13*, 2570-2580.

14. Rogina, B. et al. (2004). Sir2 mediates longevity in the fly through a pathway related to calorie restriction. Proc. Natl. Acad. Sci. USA *101*, 15998-16003.

15. Tissenbaum, H.A. et al. (2001). Increased dosage of a sir-2 gene extends lifespan in Caenorhabditis elegans. Nature *410*, 227-230.
16. Burnett, C. et al. (2011). Absence of effects of Sir2 overexpression on lifespan in C. elegans and Drosophila. Nature *477*, 482-485.
17. Herranz, D. et al. (2010). Sirt1 improves healthy ageing and protects from metabolic syndrome-associated cancer. Nat. Commun. *1*,3.
18. Oberdoerffer, P. et al. (2008). SIRT1 redistribution on chromatin promotes genomic stability but alters gene expression during aging. Cell *135*, 907-918.
19. Nogueiras, R. et al. (2012). Sirtuin 1 and sirtuin 3: physiological modulators of metabolism. Physiol. Rev. *92*, 1479-1514.
20. Kanfi, Y. et al. (2010). SIRT6 protects against pathological damage caused by diet-induced obesity. Aging Cell *9*, 162-173.
21. Kawahara, T.L. et al. (2009). SIRT6 links histone H3 lysine 9 deacetylation to NF-kappaB-dependent gene expression and organismal life span. Cell *136*, 62-74.
22. Zhong, L. et al. (2010). The histone deacetylase Sirt6 regulates glucose homeostasis via Hif1alpha. Cell *140*, 280-293.
23. Mostoslavsky, R. et al. (2006). Genomic instability and aging-like phenotype in the absence of mammalian SIRT6. Cell *124*, 315-329.
24. Kanfi, Y. et al. (2012). The sirtuin SIRT6 regulates lifespan in male mice. Nature *483*, 218-221.
25. Someya, S. et al. (2010). Sirt3 mediates reduction of oxidative damage and prevention of age-related hearing loss under caloric restriction. Cell *143*, 802-812.
26. Bahar, R. et al. (2006). Increased cell-to-cell variation in gene expression in ageing mouse heart. Nature *441*, 1011-1014.
27. de Magalhães, J.P. et al. (2009). Meta-analysis of age-related gene expression profiles identifies common signatures of aging. Bioinformatics *25*, 875-881.
28. Boulias, K. et al. (2012). The C. elegans microRNA mir-71 acts in neurons to promote germline-mediated longevity through regulation of DAF-16/FOXO. Cell Metab. *15*, 439-450.
29. Toledano, H. et al. (2012). The let-7-lmp axis regulates ageing of the Drosophilia testis stem-cell niche. Nature *485*, 605-610.

30. Ugalde, A.P. et al. (2011). Micromanaging aging with miRNAs: new messages from the nuclear envelope. Nucleus *2*, 549-555.
31. Powers, E.T. et al. (2009). Biological and chemical approaches to diseases of proteostasis deficiency. Annu. Rev. Biochem. *78*, 959-991.
32. Koga, H. et al. (2011). Protein homeostasis and aging: The importance of exquisite quality control. Ageing Res. Rev. *10*, 205-215.
33. Barzilai, N. et al. (2012). The critical role of metabolic pathways in aging. Diabetes *61*, 1315-1322.
34. Fontana, L. et al. (2010). Extending healthy lifespan- from yeast to humans. Science *328*, 321-326.
35. Colman, R.J. et al. (2009). Caloric restriction delays disease onset and mortality in rhesus monkeys. Science *325*, 201-204.
36. Schumacher, B. et al. (2008). Delayed and accelerated aging share common longevity assurance mechanisms. PLoS Genet. *4*, e1000161.
37. Garinis, G.A. et al. (2008). DNA damage and ageing: new-age ideas for an age-old problem. Nat. Cell Biol. *10*, 1241-1247.
38. Renner, O. et al. (2009). Mouse models to decipher the PI3K signaling network in human cancer. Curr. Mol. Med. *9*, 612-625.
39. Mariño, G. et al. (2010). Insulin-like growth factor 1 treatment extends longevity in a mouse model of human premature aging by restoring somatotroph axis function. Proc. Natl. Acad. Sci. USA *107*, 16268-16273.
40. Laplante, M. et al. (2009). mTOR signaling at a glance. J Cell Sci. *122*, 3589-3594.
41. Johnson, S.C. et al. (2013). mTOR is a key modulator of ageing and age-related disease. Nature *493*, 338-345.
42. Harrison, D.E. et al. (2009). Rapamycin fed late in life extends lifespan in genetically heterogeneous mice. Nature *460*, 392-395.
43. Yang, S.B. et al. (2012). Rapamycin ameliorates age-dependent obesity associated with increased mTOR signaling in hypothalamic POMC neurons. Neuron *75*, 425-436.
44. Wilkinson, J.E. et al. (2012). Rapamycin slows aging in mice. Aging Cell *11*, 675-682.
45. Salminen, A. et al. (2011). AMP-activated protein kinase (AMPK) controls the aging process via an integrated signaling network. Ageing Res. Rev. *11*, 230-241.

46. Alers, S. et al. (2012). Role of AMPK-mTOR-Ulk1/2 in the regulation of autophagy: cross talk, shortcuts, and feedbacks. Mol. Cell. Biol. *32*, 2-11.
47. Price, N.L. et al. (2012). SIRT1 is required for AMPK activation and the beneficial effects of resveratrol on mitochondrial function. Cell Metab. *15*, 675-690.
48. Fernandez-Marcos, P.J. et al. (2011). Regulation of PGC-1α, a nodal regulator of mitochondrial biogenesis. Am. J. Clin. Nutr. *93*, 884S-890S.
49. Anderson, R.M. et al. (2003). Nicotinamide and PNC1 govern lifespan extension by calorie restriction in *Saccharomyces cerevisiae*. Nature. *423*, 181-185.
50. Huynh, Frank K. et al. (2013). Targeting sirtuins for the treatment of diabetes. Diabetes Manag. *3*, 245-257.
51. Cohen, H.Y. et al. (2004). Calorie restriction promotes mammalian cell survival by inducing the SIRT1 deacetylase. Science. *305*, 390-392.
52. Banks, A.S. et al. (2008). SirT1 gain of function increases energy efficiency and prevents diabetes in mice. Cell Metab. *8*, 333-341.
53. Deng, X.Q. et al. (2007). The expression of SIRT1 in nonalcoholic fatty liver disease induced by high-fat diet in rats. Liver Int. *27*, 708-715.
54. dos Costa C.S. et al. (2010). SIRT1 transcription is decreased in visceral adipose tissue of morbidly obese patients with severe hepatic steatosis. Obes Surg. *20*, 633-639.
55. Purushotham, A. et al. (2012). Systemic SIRT1 insufficiency results in disruption of energy homeostasis and steroid hormone metabolism upon high-fat diet feeding. FASEB J. *26*, 656-667.
56. Xu, F. et al. (2010). Lack of SIRT1 (Mammalian Sirtuin 1) activity leads to liver steatosis in the $SIRT1^{+/-}$ mice: a role of lipid mobilization and inflammation. Endocrinology. *151*, 2504-2514.
57. Bordone, L. et al. (2007). SIRT1 transgenic mice show phenotypes resembling calorie restriction. *6*, 759-767.
58. Takaoka, M.J. et al. (1940). Of the phenolic substances of white hellebore (*Veratrum grandiflorum* Loes. fil.). J Faculty Sci Hokkaido Imp Univ. *3*, 1-16.
59. Nonomura, S. et al. (1963). Constituents of polygonaceous plants. I Studies on the components of Ko-jo-kon (*Polygonum cuspidatum* Sieb et Zucc.). Yakugaku Zasshi. *83*, 988-990.

60. Arichi, H. et al. (1982). Effects of stilbene components of the roots of Polygonum cuspidatum Sieb et Zucc on lipid metabolism. Chem Pharm Bull. *30*, 1766-1770.
61. Siemann, E.H. et al. (1992). Concentration of the phytoalexin resveratrol in wine. Am J Enol Vitic. *43*, 49-52.
62. Baur, J.A. et al. (2006). Resveratrol improves health and survival of mice on a high-calorie diet. Nature. *444*, 337-342.
63. Ramadori, G. et al. (2009). Central administration of resveratrol improves diet-induced diabetes. Endocrinology. *150*, 5326-5333.
64. Rocha, K.K. et al. (2009). Resveratrol toxicity: effects on risk factors for atherosclerosis and hepatic oxidative stress in standard and high-fat diets. Food Chem Toxicol. *47*, 1362-1367.
65. Deng, J.Y. et al. (2008). Activation of estrogen receptor is crucial for resveratrol-stimulating muscular glucose uptake via both insulin-dependent and –independent pathways. Diabetes. 57, 1814-1823.
66. Palsamy, P. et al. (2008). Resveratrol, a natural phytoalexin, normalizes hyperglycemia in streptozotocin-nicotinamide induced experimental diabetic rats. Biomed Pharmacother. *62*, 598-605.
67. Poulsen, M.M. et al. (2012). Resveratrol up-regulates hepatic uncoupling protein 2 and prevents development of nonalcoholic fatty liver disease in rats fed a high-fat diet. Nutr Res. *32*, 701-708.
68. Vang, O. et al. (2011). What is new for an old molecule? Systematic review and recommendation on the use of resveratrol. PLoS One. 6:e19881.
69. Eliott, P.J. et al. (2009). Resveratrol/SRT-501. Drugs Fut. *34*, 291.
70. Yoshino, J. et al. (2012). Resveratrol supplementation does not improve metabolic function in nonobese women with normal glucose tolerance. Cell Metab. *16*, 658-664.
71. Poulsen, M.M. et al. (2012). High-dose resveratrol supplementation in obese men: an investigator-initiated, randomized, placebo-controlled clinical trial of substrate metabolism, insulin sensitivity, and body composition. Diabetes. *62*, 1186-1195.
72. Timmers, S. et al. (2011). Calorie restriction-like effects of 30 days of resveratrol supplementation on energy metabolism and metabolic profile in obese humans. Cell Metab. *14*, 612-622.

73. Brown, V.A. et al. (2010). Repeat dose study of the cancer chemopreventive agent resveratrol in healthy volunteers: safety, pharmacokinetics, and effect on the insulin-like growth factor axis. Cancer Res. *70*, 9003-9011.
74. Howitz, K.T. et al. (2003). Small molecule activators of sirtuins extend Saccharomyces cerevisiae lifespan. Nature. *425*, 191-196.
75. Park SJ. et al. (2012). Resveratrol ameliorates aging-related metabolic phenotypes by inhibiting cAMP phosphodiesterases. Cell. *148*, 421–433.
76. Hubbard BP. et al. (2013). Evidence for a common mechanism of SIRT1 regulation by allosteric activators. Science. *339*, 1216–1219.
77. Guarante, Leonard. (2014). Calorie restriction and sirtuins revisited. Genes & Development. *27*, 2072-2085.
78. McCay CM. et al. (1935). The effect of retarded growth upon the length of the life span and upon the ultimate body size. J Nutr. *10*, 63–73.
79. Lin SJ. et al. (2000). Requirement of NAD and SIR2 for life-span extension by calorie restriction in *Saccharomyces cerevisiae*. Science. *289*, 2126–2128.
80. Kaeberlein M. et al. (2004). Sir2-independent life span extension by calorie restriction in yeast. PLoS Biol. *2*, E296.
81. Chalkiadaki A, Guarente L. (2012). High-fat diet triggers inflammation-induced cleavage of SIRT1 in adipose tissue to promote metabolic dysfunction. Cell Metab. *16*, 180–188.
82. Pedersen SB. et al. (2008). Low Sirt1 expression, which is upregulated by fasting, in human adipose tissue from obese women. Int J Obes (Lond). *32*, 1250–1255.
83. Chen D. et al. (2005). Increase in activity during calorie restriction requires Sirt1. Science. *310*, 1641.
84. Lagouge M. et al. (2006). Resveratrol improves mitochondrial function and protects against metabolic disease by activating SIRT1 and PGC-1α. Cell. *127*, 1109–112.
85. Pfluger PT. et al. (2008). Sirt1 protects against high-fat diet-induced metabolic damage. Proc Natl Acad Sci. *105*, 9793–9798.
86. Guarente L. et al. (2011). Sirtuins, aging, and medicine. N Engl J Med *364*: 2235–2244.

87. Yin, X. et al. (2013). Niche-independent high-purity cultures of Lgr5^{+} intestinal stem cells and their progeny. Nature Methods. *10*, 1038.

88. Cao, Li. et al. (2013). Development of Intestinal Organoids as Tissue Surrogates: Cell Composition and the Epigenetic Control of Differentiation. Molecular Carcinogenesis. *10*, 1002.

89. Holloway, K. et al. (2010). SIRT1 regulates Dishevelled proteins and promotes transient and constitutive Wnt signaling. PNAS. *107*, 9216-9221.

90. Textbook: Weinberg, Robert A. The Biology of Cancer. Taylor & Francis, 2006.

91. Electronic: SIRT1 inactivation reduces tumor growth in colon cancer model. http://www.fredhutch.org/en/news/spotlight/imports/sirt1-inactivation-reduces-tumor-growth-in-colon-cancer-model.html.

92. Leko, V. et al. (2013). Enterocyte-Specific Inactivation of SIRT1 Reduces Tumor Load in the APC$^{+/min}$ Mouse Model. PLOS ONE. *8*, e66283.

93. Herranz, D. et al. (2012). SIRT1 promotes thyroid carcinogenesis driven by PTEN deficiency. Oncogene.

94. Song, NY. et al. (2012). Janus-faced role of SIRT in tumorigenesis. Ann N Y Acad Sci. *1271*, 10-19.

95. Su, LK. et al. (1992). Multiple intestinal neoplasia caused by a mutation in the murine homolog of the APC gene. Science. *256*, 668-670.

96. Rubinfeld, B. et al. (1993). Association of the APC gene product with beta-catenin. Science. *262*, 1731-1734.

97. Munemitsu, S. et al. (1995). Regulation of intracellular beta-catenin levels by the adenomatous polyposis coli (APC) tumor-suppressor protein. Proc Natl Acad Sci U S A. *92*, 3046-3050.

98. Firestein, R. et al. (2008). The SIRT1 deacetylase suppresses intestinal tumorigensis and colon cancer growth. PLoS One. *3*, e2020.

99. Boily, G. et al. (2009). SirT1- null mice develop tumors at normal rates but are poorly protected by resveratrol. Oncogene. *28*, 2882-2893.

100. User Manual: ClonTech Laboratories. Macherey-Nagel. Plasmid DNA Purification. 2012. Rev. 10.

101. Alcendor, R.R.. et al. (2007). Sirt1 regulates aging and resistance to oxidative stress

in the heart. Circ. Res. *100*, 1512-1521.

102. Kakefuda, K. et al. (2009). Sirtuin 1 overexpression mice show a reference memory deficit, but not neuroprotection. Biochem. Biophys. Res. Commun. *387*, 784-788.

103. Sato T, Vries RG, Snippert HJ, van de Wetering M, Barker N, Stange DE, van Es JH, Abo A, Kujala P, Peters PJ, Clevers H. (2009). Single Lgr5 stem cells build crypt-villus structures in vitro without a mesenchymal niche. Nature. 459(7244):262-5.

104. Barker N, van Es JH, Kuipers J, Kujala P, van den Born M, Cozijnsen M, Haegebarth A, Korving J, Begthel H, Peters PJ, Clevers H. (2007). Identification of stem cells in small intestine and colon by marker gene Lgr5. Nature. 449(7165):1003-7.

105. Sato T. et al. (2010). Paneth cells constitute the niche for Lgr5 stem cells in intestinal crypts. Nature. 469(7330):415-8.

106. Sasso G. et al. (2014). Loss of Sirt1 Function Improves Intestinal Anti-Bacterial Defense and Protects from Colitis-Induced Colorectal Cancer. PLOS. 10.1371/journal.pone.0102495.

107. Daniel M. et al. (2015). Epigenetic linkage of aging, cancer and nutrition. J Exp Biol. 2015 Jan 1;218(Pt 1):59-70.